Stream temperature under contrasting riparian forest cover

Dugdale, Stephen J.; Malcolm, Iain A.; Kantola, Kaisa; Hannah, David M.

DOI:
10.1016/j.scitotenv.2017.08.198

Science of the Total Environment 610–611 (2018) 1375–1389

Contents lists available at ScienceDirect

Science of the Total Environment

journal homepage: www.elsevier.com/locate/scitotenv

Stream temperature under contrasting riparian forest cover: Understanding thermal dynamics and heat exchange processes

Stephen J. Dugdale [a,*], Iain A. Malcolm [b], Kaisa Kantola [a], David M. Hannah [a]

[a] School of Geography, Earth and Environmental Sciences, University of Birmingham, Edgbaston, Birmingham B15 2TT, United Kingdom
[b] Marine Scotland Science, Freshwater Fisheries Laboratory, Faskally, Pitlochry PH16 5LB, United Kingdom

HIGHLIGHTS

- We assess stream temperature and energy fluxes under 3 riparian vegetation types.
- Stream temperature varies significantly between different vegetation types.
- Net energy fluxes are greatest in open grassland and lowest in coniferous woodland.
- Results of this study have implications for riparian tree planting schemes.

GRAPHICAL ABSTRACT

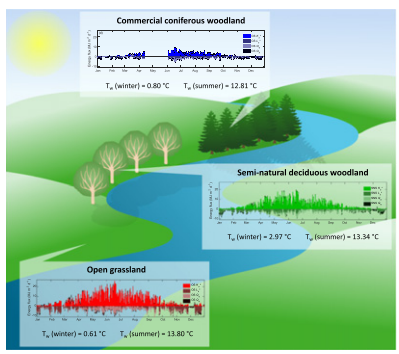

ARTICLE INFO

Article history:
Received 4 July 2017
Received in revised form 18 August 2017
Accepted 18 August 2017
Available online 30 August 2017

Editor: D. Barcelo

Keywords:
River temperature
Riparian shading
Forest
Energy balance
Climate change

ABSTRACT

Climate change is likely to increase summer temperatures in many river environments, raising concerns that this will reduce their thermal suitability for a range of freshwater fish species. As a result, river managers have pursued riparian tree planting due to its ability to moderate stream temperatures by providing shading. However, little is known about the relative ability of different riparian forest types to moderate stream temperatures. Further research is therefore necessary to inform best-practise riparian tree planting strategies. This article contrasts stream temperature and energy fluxes under three riparian vegetation types common to Europe: open grassland terrain (OS), semi-natural deciduous woodland (SNS), and commercial conifer plantation (CS). Data was recorded over the course of a year by weather stations installed in each of the vegetation types. Mean daily stream temperature was generally warmest at OS and coolest at CS. Energy gains at all sites were dominated by shortwave radiation, whereas losses where principally due to longwave and latent heat flux. The magnitude of shortwave radiation received at the water surface was strongly dependent upon vegetation type, with OS and SNS woodland sites receiving approximately 6× and 4× (respectively) the incoming solar radiation of CS. Although CS lost less energy through longwave or latent fluxes than the other sites, net surface heat flux was ordered OS > SNS > CS, mirroring the stream temperature results. These findings demonstrate that energy fluxes at the air-water interface vary substantially between different riparian forest types and that stream temperature response to bankside vegetation depends upon the type of vegetation present. These results present new insights into the conditions under which riparian vegetation shading is optimal for the reduction of surface heat fluxes and have important implications for the development of 'best-practice' tree planting strategies to moderate summer temperature extremes in rivers.

* Corresponding author.
E-mail address: s.j.dugdale@bham.ac.uk (S.J. Dugdale).

http://dx.doi.org/10.1016/j.scitotenv.2017.08.198

1. Introduction

Water temperature is one of the principal river habitat variables, exerting an influence on chemical, physical and biological processes within the river channel (e.g. Caissie, 2006). River temperature is therefore important to freshwater fish species, many of which inhabit relatively tight thermal niches (e.g. Jonsson and Jonsson, 2009). In addition to influencing levels of growth and survival, river temperatures can alter behaviour and drive mortality events, eventually leading to population decline (Breau et al., 2011; Dugdale et al., 2016; Martins et al., 2012). Even under conservative emissions scenarios (see IPCC, 2013), most global climate models indicate that global river temperatures will increase by ~1.0–3.0 °C (Ficke et al., 2007; Morrill et al., 2005; van Vliet et al., 2013; van Vliet et al., 2011) by 2070–2100. Although the magnitude of temperature increase will inevitably vary between locations, large temperature rises are expected in some northern European watersheds (e.g. van Vliet et al., 2011; Webb, 1996) where temperature-sensitive fish species are often resident. Within these locations, exposed upland streams such as those in Scotland will be particularly susceptible to warming due to their relatively low thermal inertia (in comparison to larger rivers) and their lack of substantial shading (e.g. Hrachowitz et al., 2010; Jackson et al., 2017). Indeed, recent research suggests that temperatures in Scottish upland rivers could increase by an average of 2.2 °C by 2050 alone (Capell et al., 2013; Punzet et al., 2012), and the high degree of exposure of large tracts of Scottish rivers (forest cover in Scotland is only 17.1%; Forestry Commission Scotland, 2006) means that such a warming could have serious impacts on Scotland's fluvial ecosystems. Research is therefore needed to help understand and mitigate river temperature extremes in these exposed upland environments.

Over the past twenty years a large number of river temperature studies have provided valuable insights into the dominant processes driving river temperature regimes (e.g. Caissie, 2006; Hannah and Garner, 2015; Webb et al., 2008). At the largest scales, temperature is controlled by energy fluxes at the air-water and streambed interfaces (Caissie, 2006; Webb, 1996). Although advective and sensible heat fluxes at these interfaces exert an influence on river temperature (Webb and Zhang, 2004; Yearsley, 2009), radiative and evaporative fluxes at the water surface are generally considered the dominant heat exchange mechanisms (Caissie, 2006; Caissie, 2016; Maheu et al., 2014; Morin and Couillard, 1990). While the role of these heat fluxes in determining stream temperature is reasonably well understood, the magnitude and direction of energy transfer processes can be substantially altered by the properties of the landscape through which the river flows (e.g. Benyahya et al., 2012; Dugdale et al., 2015; Garner et al., 2014; Leach and Moore, 2010). Indeed, the degree to which a river responds to radiative and climatic forcing is heavily dependent on patterns of land use and topography within the basin, and is thus complex and multi-faceted (Hannah and Garner, 2015; Laizé and Hannah, 2010).

Despite the difficulty in elucidating many of the landscape properties controlling river temperature, some landscape - river temperature interactions have long been recognised. For example, experiments conducted during forest clearcutting since the early 1970s have demonstrated how the removal of riparian vegetation can result in greatly increased summer water temperatures under some circumstances (e.g. Brown and Krygier, 1970; Burton and Likens, 1973; Keith et al., 1998; Moore et al., 2005a; Rishel et al., 1982; Roth et al., 2010; Zwieniecki and Newton, 1999). Given the reasonable assumption that the addition of new riparian vegetation will have the opposite effect, river managers have started to pursue riparian tree planting as a strategy for moderating high temperature events in summer (e.g. Drainey, 2012; EA, 2011; Lawrence and Dandy, 2014; Lowe et al., 2012; Parrott and Holbrook, 2006; Withrow-Robinson et al., 2011). However, it is only recently that studies have started to identify the precise manner by which riparian tree cover causes an apparent cooling effect on river channels (see Garner et al., 2014). Furthermore, while previous research has documented how stream temperature (and corresponding energy fluxes) can differ between forested and exposed river reaches (e.g. Garner et al., 2015; Hannah et al., 2008; Leach and Moore, 2010; Webb and Zhang, 1997, 1999, 2004), little is known about how stream temperature dynamics respond to variability in riparian forest cover or species. Indeed, while the majority of previous studies (reviewed in Moore et al., 2005a) have concentrated on the impact of dense riparian conifer woodland on river temperature, riparian planting is increasingly focused around achieving multiple environmental benefits, and semi-natural deciduous riparian woodland plantation is instead often preferred in the UK. There is therefore a pressing need to quantify how riparian energy fluxes respond to differing forest types in order to better understand the impact of different tree plantation strategies on stream temperature dynamics with a view to improved climate change mitigation.

This paper therefore presents a detailed comparison of stream temperatures and energy fluxes associated with three different riparian vegetation types in Loch Ard Forest, Scotland. First, we characterise spatial and temporal variability in stream water temperature regimes between open grassland, semi-natural deciduous and commercially-planted coniferous forested reaches of three streams. We then examine differences in energy fluxes under the three forest cover types. Finally, we assess how observed variations in energy fluxes are responsible for the observed patterns of stream temperature, with a view to understanding the physical processes driving stream temperature regimes under varying forest cover. We hypothesise that stream temperature regimes and energy fluxes will differ significantly between different forest treatments and that variability in these parameters will be largely driven by alterations in the amount of solar radiation received at each site as a result of contrasting riparian shading.

2. Methodology

2.1. Study area

Loch Ard is a forest park situated between Loch Lomond and Aberfoyle (districts of Argyll & Bute and Stirling) on the west coast of Scotland (Fig. 1). The park is home to a long-term monitoring programme by Marine Scotland Science (started 1976) and has hosted a variety of studies on hydrology, hydrochemistry, acidification, freshwater fish and invertebrates (e.g. Harriman et al., 1995; Harriman et al., 2003; Malcolm et al., 2014; McCartney et al., 2003; Tetzlaff et al., 2007). The park contains a range of different riparian vegetation types, ranging from open grassland to both semi-natural deciduous and commercially-planted conifer woodland (Forestry Commission Scotland, 2015). Geology within the area is dominated by low-permeability metamorphic bedrock covered by slow-draining peaty gleys and podsols (Tetzlaff et al., 2007). The area is subject to high levels of precipitation, receiving an average of 1980 mm per year (Tetzlaff et al., 2007). Winters are relatively mild for the latitude (mean January air temperature of 2.8 °C) although mean summer air temperatures also remain low (mean of 13.7 °C; Tetzlaff et al., 2010). Although snowfall does occur in winter, it is usually a relatively minor component of the annual hydrograph (Tetzlaff et al., 2010).

Within the forest park, three sites comprising stream reaches with different forest cover types were selected to contrast variability water temperature and energy fluxes. One grassland site was clear of any significant forest cover and was thus used as a control; the remaining two were chosen to characterise two riparian forest types typically found in Scotland: semi-natural broadleaf and commercial non-indigenous conifer. The control site (termed OS (open site) hereafter; plotted in red) was characterised by open (exposed) riparian grassland with no significant canopy cover. Clear felling within the 10-year period prior to this study ensured that no vegetation taller than ~1 m existed within the riparian zone, where herbaceous plants/shrubs dominate. The OS sub-

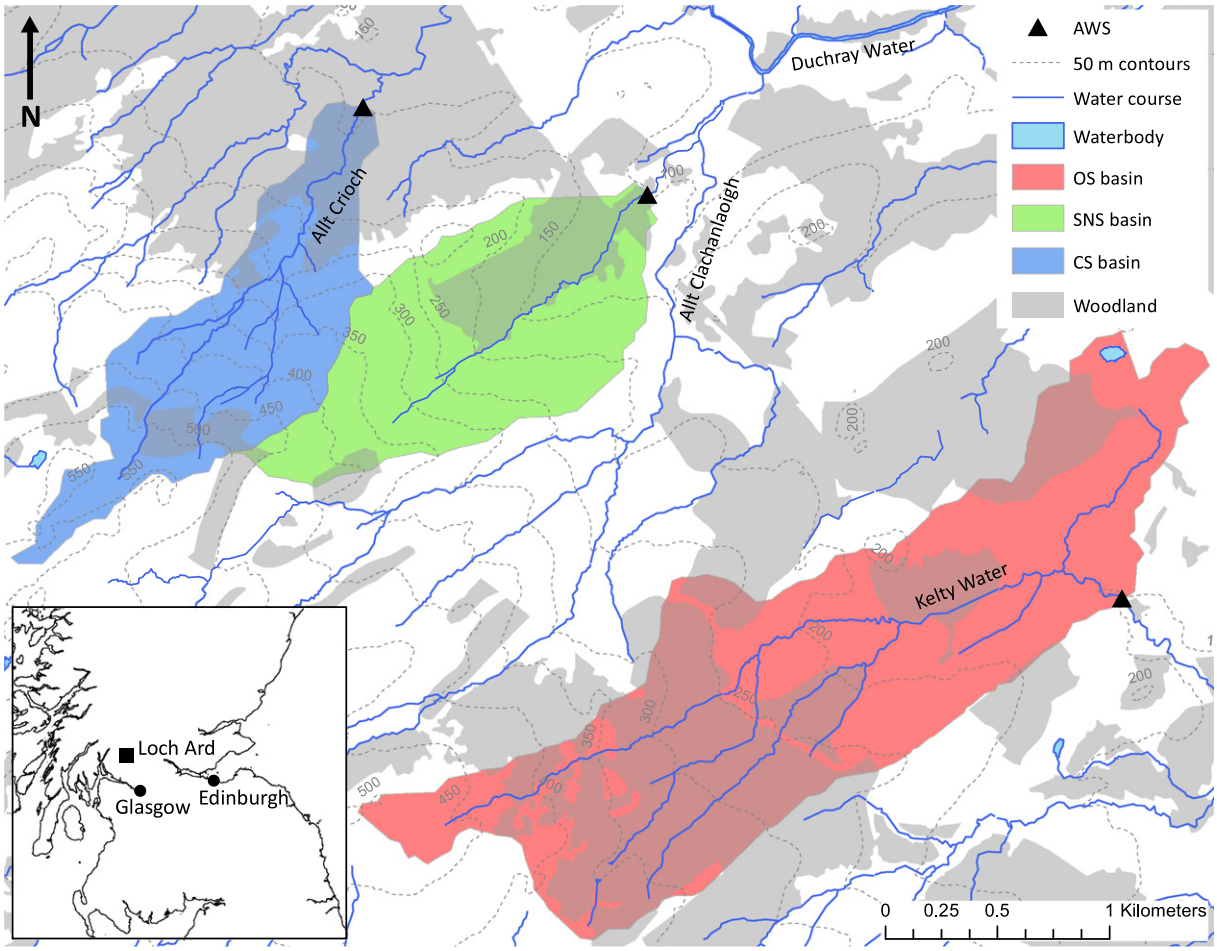

Fig. 1. Section of Loch Ard Forest Park containing study sites OS (open grassland), SNS (semi-natural woodland) and CS (commercial coniferous woodland).

basin covers approximately 3.1 km^2 with an average altitude of 253 m. The semi-natural forest site (termed SNS hereafter; plotted in green) was characterised by mixed native deciduous species (birch, rowan and alder; approximate heights 10–20 m) growing directly on the stream banks. The SNS sub-basin covers approximately 1.3 km^2 with a mean altitude of 243 m. The commercial conifer plantation site (termed CS hereafter; plotted in blue) comprised Sitka spruce monoculture originally planted in 1978 (approximate heights 40–50 m). Mean altitude for the CS sub-basin was 367 m, with a basin area of 1.17 km^2. The active channel width for all study reaches varied between 1.3 m and 1.5 m. The SNS and CS study reaches were oriented in the same approximate SW – NE direction. Although OS was oriented NW-SE, it is unlikely that this orientation will substantially alter energy fluxes in relation to SNS and CS because of the lack of riparian vegetation. Mean discharge at OS and CS (recorded from stage-discharge curves established between pressure transducers installed at the sites and a nearby gauging station) was 0.09 and 0.08 m^3 s^{-1} respectively. Although no pressure transducer was available for the SNS sub-basin, its similar size and location near to CS means that its hydrometric regime (i.e. average discharge) is very similar.

2.2. Field data collection

A range of measurements necessary to characterise the stream temperature regime and energy fluxes at each site were collected between 1st January and 31st December 2010. Automated weather stations (AWS) installed above the stream at each site were used to collect data following methods described by Hannah et al. (2004). Stream temperature (T_w) measurements were obtained from thermistors anchored in the water column and protected from the effects of sunlight by PVC tubing. Direct measures of incoming ($K_s\downarrow$) and reflected shortwave radiation ($K_s\uparrow$) and net radiation (Q^*) were used to characterise radiative fluxes at the water surface, while air temperature (T_a), relative humidity (RH), wind speed (WS) were recorded in order to compute latent (Q_e) and sensible (Q_h) heat exchanges (see Section 2.3). Bed heat flux (Q_{bhf}) and bed shortwave radiation ($K_b\downarrow$) were measured using instrumentation installed within the channel bed, while stream bed temperatures (T_b; measured using thermistors buried at 0.05 m, 0.20 m and 0.40 m) were used to compute new streambed longwave flux ($L_b{}^*$; see Section 2.3). A complete list of variables (and instruments used to collect the data) is given in Table 1. All instruments were cross-calibrated prior to installation and found to be in good agreement. Instruments were polled at 10 s intervals and mean values (maximum for relative humidity) logged at 15 min intervals. The automated weather stations (AWS) were serviced and downloaded at approximately 6-week intervals.

All data for CS between 14th April and 3rd June were lost due to battery failure. Bed radiation ($K_b\downarrow$) data were rejected on several occasions where high flows following precipitation events had dislodged the pyrometer. Bed heat flux (Q_{bhf}) values at CS between 15th July and 31st December were found to be erroneous and were removed from the dataset. Streambed temperature (T_b) data at 0.40 m at OS were discarded due to a sensor fault that persisted over the duration of the study; a similar problem led to the rejection of bed temperature data at 0.05 m from SNS between 1st January and 30th May. Instruments were periodically obstructed following high snowfall/precipitation events; these periods were identified in the measurement time-series and removed from subsequent analysis.

Table 1
Hydrometeorological variables collected at automated weather stations (AWS).

Variable	Instrument	Location	Instrument error
Stream temperature (T_w)	Campbell Scientific 107 thermistor	0.05 m above streambed	±0.2 °C
Stream bed temperature (T_b)	Campbell Scientific 107 thermistor	0.05, 0.20, 0.40 m below stream bed	±0.2 °C
Air temperature (T_a) and relative humidity (RH)	Vaisala HMP45C temperature/relative humidity probe	~2.00 m above stream surface	Temperature ± 0.4 °C, RH ± 3%
Wind speed (WS)	Vector Instruments A100R 3-cup anemometer	~2.00 m above stream surface	±1% + 0.1 m s^{-1}
Incoming ($K_s\downarrow$) and reflected ($K_s\uparrow$) solar shortwave radiation	Skye SKS 1110 pyranometer	~1.75 m above stream surface	±5%
Bed shortwave radiation ($K_b\downarrow$)	Skye SKS 1110 pyranometer	Streambed surface	±5%
Net all-wave radiation (Q^*)	Kipp & Zonen NR Lite net radiometer (OS and CS), REBS Q5 net radiometer (SNS)	~1.75 m above stream surface	±5% (NR Lite & REBS Q5)
Bed heat flux (Q_{bhf})	Hukseflux HFP01 soil heat flux plate	0.05 m below stream bed	3%

2.3. Stream energy balance

Webb and Zhang (1997) express the energy budget of a stream not receiving significant inflow as:

$$Q_n = Q^* + Q_h + Q_e + Q_b + Q_f + Q_a$$

where Q_n is the total energy flux, Q^* is the net radiative flux (all wavelengths), Q_h is the sensible heat flux, Q_e is the latent heat flux, Q_b is the energy flux from bed conduction, Q_f is the energy flux resulting from friction with the bed and banks and Q_a is the advective heat flux resulting from runoff and/or groundwater inputs. Fluid friction in this study was considered to be negligible and was omitted from the energy budget calculation. Similarly, in the absence of data regarding advective groundwater/runoff inputs, Q_b and Q_a were substituted with Q_{bhf} which aggregates conductive, convective, radiative and advective processes at the stream bed (Hannah et al., 2004). The stream energy budget at each of the three sites was thus based on the following modified equation:

$$Q_n = Q^* + Q_h + Q_e + Q_{bhf}$$

The following flux terms needed to complete the energy budget at each site were measured or estimated from data observed at the three AWS, according to the methods detailed in Hannah et al. (2004, 2008):

1. Net short-wave ($K_s{}^*$) and net long-wave ($L_s{}^*$) radiation at the stream–air interface.
2. Streambed net short wave ($K_b{}^*$), net long wave ($L_b{}^*$), and net all-wave streambed radiation ($Q_b{}^*$).
3. Latent heat flux (Q_e), using a Dalton-style equation to derive heat lost by evaporation or gain by condensation (Evans et al., 1998; Webb and Zhang, 1997).
4. Sensible heat flux (Q_h), as a product of Q_e and the Bowen ratio (Bowen, 1926).

All energy fluxes are subsequently reported in MJ m^2 d^{-1} and are positive (negative) when adding (removing) heat to (from) the water column.

2.4. Data analysis

Patterns in stream temperature and energy fluxes are examined both in terms of annual and seasonal (winter and summer) timescales. Although plots/tables show data for the entire year, sporadic data gaps during spring and autumn made analysis of patterns during these seasons difficult. We therefore focus on the winter and summer months because a) data availability was greatest during these time periods and b) winter and summer are of high importance from a biological perspective (e.g. Dugdale et al., 2016; Wirth et al., 2012). Furthermore, contrasts between sites were maximised during the winter and summer seasons, making inter-site differences more readily apparent. For the purposes of this study, winter was defined as December, January and February and summer was defined as June – August. Where data was missing at one or more sites, descriptive statistics and data analyses were only calculated using concomitant data from all three sites, meaning that like-for-like comparisons between sites are valid.

Preliminary analyses (Durbin-Watson tests, examination of autocorrelation/partial autocorrelation plots; see Dickson et al., 2012) revealed serial autocorrelation of all timeseries. Significance of inter-site differences was therefore quantified using a mixed-effects analysis-of-variance (ANOVA) incorporating a first-order autocorrelation (AR1) process; this ensured that the reporting of significant differences between sites was not influenced by the autocorrelation of residuals. The strength of association between pairs of variables (e.g. air and water temperature) was assessed using the coefficient of determination of linear regression (R^2). In order to account for the effect of serial autocorrelation on the linear regression, autoregressive integrated moving average (ARIMA) models (e.g. Benyahya et al., 2007; Gurnell et al., 1992) were fitted to each variable; linear regressions were subsequently established between the ARIMA model residuals, effectively removing the influence of autocorrelation.

3. Results

3.1. Stream temperature

Stream temperature was significantly different across the three sites (mixed-effects ANOVA $p < 0.01$). Averaged across the study period, mean daily stream temperature was warmest at the semi-natural forest site (SNS; 7.6 °C) and coolest in the commercial conifer plantation (CS; 6.5 °C). However, despite SNS yielding higher average temperatures, OS (control open grassland site) attained both the highest summer (June–August) and coolest winter (December–February) daily mean temperature (13.8 °C and 0.6 °C respectively). Stream temperature at OS was also the most variable, as demonstrated by the relatively high standard deviation (5.7 °C) compared to SNS or CS (Table 2). Inter-site differences in stream temperature also varied between seasons (Fig. 2a). While in the summer, daily mean temperatures are consistently ordered OS > SNS > CS (13.8, 13.3 and 12.8 °C respectively), a transition occurs in the cooler months, meaning that in winter, SNS is considerably warmer (3.0 °C) than OS or CS (0.6 and 0.8 °C respectively). This temperature difference is presumably due (in part) to the effects of winter ice formation at OS and CS which was not replicated at SNS. Diurnal stream temperature dynamics follow a similar but modified annual cycle (Fig. 2b–d). In summer, OS consistently records the greatest mean daily temperature range (4.1 °C), followed by CS (3.4 °C) and SNS (3.1 °C). However, during winter, the mean daily temperature range at SNS (1.0 °C) is higher than either OS or CS (0.6 and 0.7 °C), presumably a function of the substantially higher winter stream temperatures at this site. Stream temperature was moderately well correlated to air temperature (T_a; Supplementary material; Fig. S1a, Table S1) at all sites ($R^2 = 0.61$, 0.49 and 0.40 respectively for CS, SNS and OS respectively). However,

Table 2
Descriptive statistics (daily mean, minimum, maximum and standard deviation) for stream temperature.

		Annual				Winter				Summer			
Variable	Site	Mean	Min	Max	SD	Mean	Min	Max	SD	Mean	Min	Max	SD
T_w (°C)	OS	6.8	−0.3	17.5	5.7	0.6	−0.3	3.9	0.9	13.8	10.5	17.5	1.6
T_w (°C)	SNS	7.6	−0.1	15.8	4.7	3.0	−0.1	5.1	1.0	13.3	10.9	15.8	1.1
T_w (°C)	CS	6.5	−0.1	15.8	5.2	0.8	−0.1	4.0	1.1	12.8	9.4	15.8	1.3

the decreasing correlation strength from CS to OS indicates that air temperature explains increasingly less variability in stream temperature as tree cover decreases.

3.2. Energy fluxes at the air-water interface

Seasonal variability in solar shortwave and longwave radiation means that net radiation is characterised by a strong annual cycle, whereby Q^* represents a heat sink (due to outgoing longwave radiation) in winter and a substantial heat source (incident shortwave) during warmer months. In terms of net solar shortwave radiation (K_s^*), minimum and maximum values track the winter and summer solstices (Fig. 3a); outside of the spring/autumn equinoxes, incident shortwave radiation at all sites generally drops below 20% of the summer maximum. Clear inter-site trends are present in the K_s^* observations. OS recorded the highest average value (6.3 MJ m^2 d^{-1}) followed by SNS (4.3 MJ m^2 d^{-1}) and CS (2.0 MJ m^2 d^{-1}); these inter-site differences were significant ($p < 0.01$). Clear seasonal trends are also visible in the solar radiation differences between the three sites (Table 3). While SNS and CS receive ~67% and 34% of the total radiation of OS during summer,

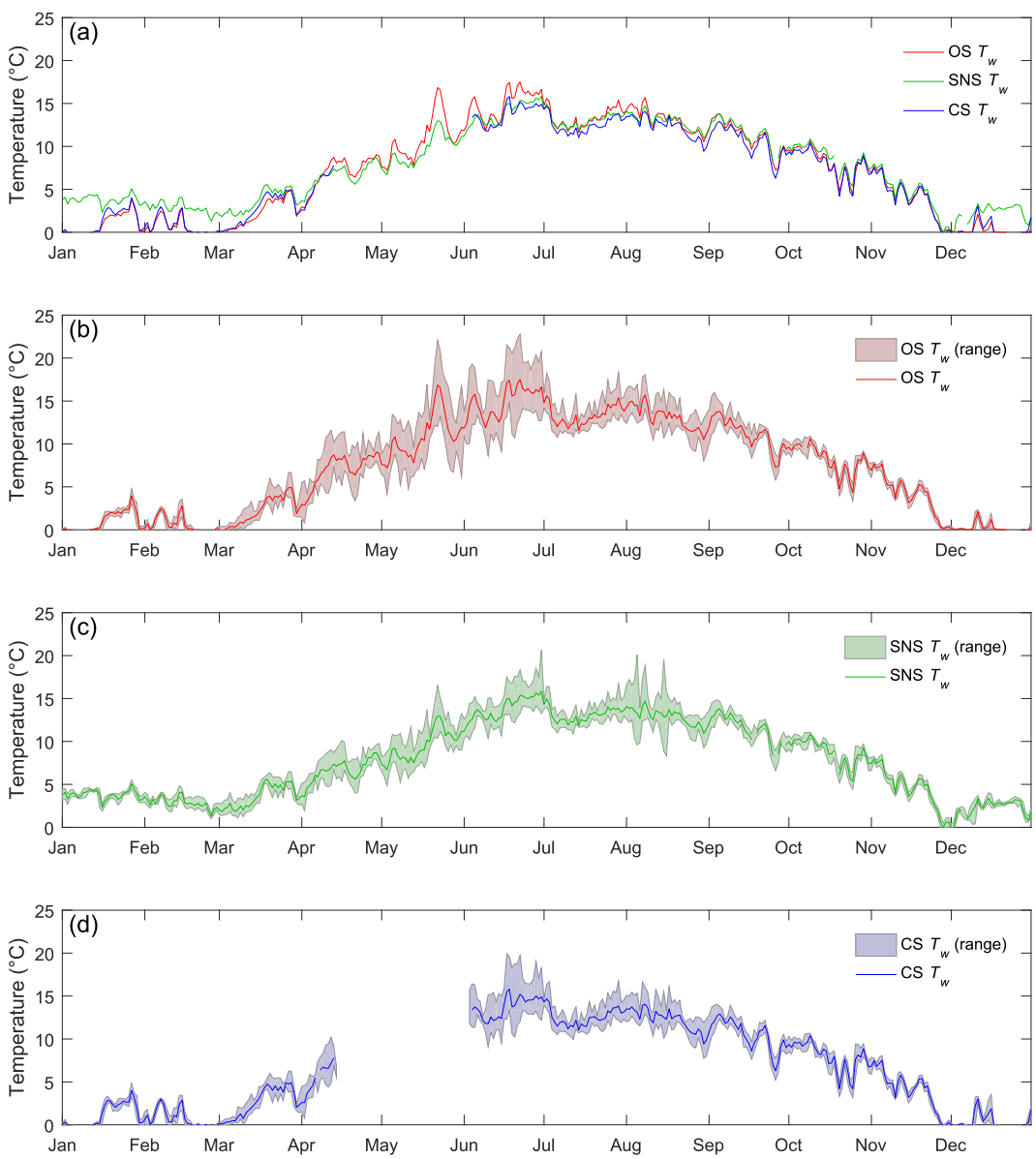

Fig. 2. (A) Daily mean stream temperature recorded by AWS. (B)–(D) Daily mean temperature superimposed on daily range at (B) OS (open grassland), (C) SNS (semi-natural woodland) and (D) CS (commercial coniferous woodland), allowing for visualisation of stream temperature maxima/minima.

the difference between OS and SNS/CS is further increased during the winter months (with SNS and CS only receiving 53% and 19% respectively of the radiation at OS).

Averaged over the year, net longwave radiation (L_s*) is a heat sink at all sites (−2.2, −1.3 and −1.2 MJ m^2 d^{-1} respectively for OS, SNS and CS; Table 3). Results of the mixed-effects ANOVA indicate that there is no significant difference in mean net longwave radiation across the three sites. However, visual inspection of the data indicates some weak site-dependent seasonal patterns (Fig. 3b). OS is characterised by a pronounced annual cycle, whereby energy loss from L_s* is substantially reduced in summer ($\bar{x}$ = −0.5 MJ m^2 d^{-1}) compared to winter ($\bar{x}$ = −4.1 MJ m^2 d^{-1}). Conversely, CS and SNS exhibit much reduced seasonal variability. While SNS records a similar pattern of greater L_s* losses in winter than in summer (−1.7 (winter) vs −1.2 (summer) MJ m^2 d^{-1}), this pattern is inverted at CS, where most energy is lost in summer (−1.4 (summer) vs −1.1 (winter) MJ m2d^{-1}). Despite the relative seasonal stability of CS (and to a lesser extent, SNS), absolute differences in L_s* among all three sites show clear seasonal trends, with differences maximised around the annual solstices and minimised during the equinoxes.

Latent heat contributes almost exclusively to heat loss (Table 3) at all sites with the exception of isolated occasions whereby Q_e-driven energy gains (condensation) occur either due to winter ice cover or during occasions when high relative humidity (Fig. S1b, Table S1) coincides with elevated air-water temperature gradients (Fig. 3c). This is supported by the moderate (significant) correlation between relative humidity and Q_e at all sites (R^2 = 0.53, 0.57 and 0.54 at OS, SNS and CS respectively). Over the course of the year, average heat loss due to Q_e is greatest at OS (−1.5 MJ m2d^{-1}), followed by SNS (−1.0 MJ m^2 d^{-1}) and CS (−0.4 MJ m^2 d^{-1}); these differences were found to be significant (p < 0.01). No significant difference in air temperature (T_a) was observed between the three sites, so the inter-site ordering of latent heat losses are likely due to differences in humidity (81 ± 8%, 82 ± 7% and 89 ± 7% for OS, CS and SNS respectively) and wind speed (1.0 ± 0.7 m s^{-1}, 0.4 ± 0.3 m s^{-1} and 0.1 ± 0.1 m s^{-1} for OS, CS and SNS respectively; Fig. S1c, Table S1) whereby increased wind speed and decreased humidity enhance evaporation. A strong seasonal cycle is present at all sites, whereby Q_e heat losses are maximised in the summer and minimised in the winter. Inter-site differences also track the same annual cycle whereby differences between the three sites are generally low (<±

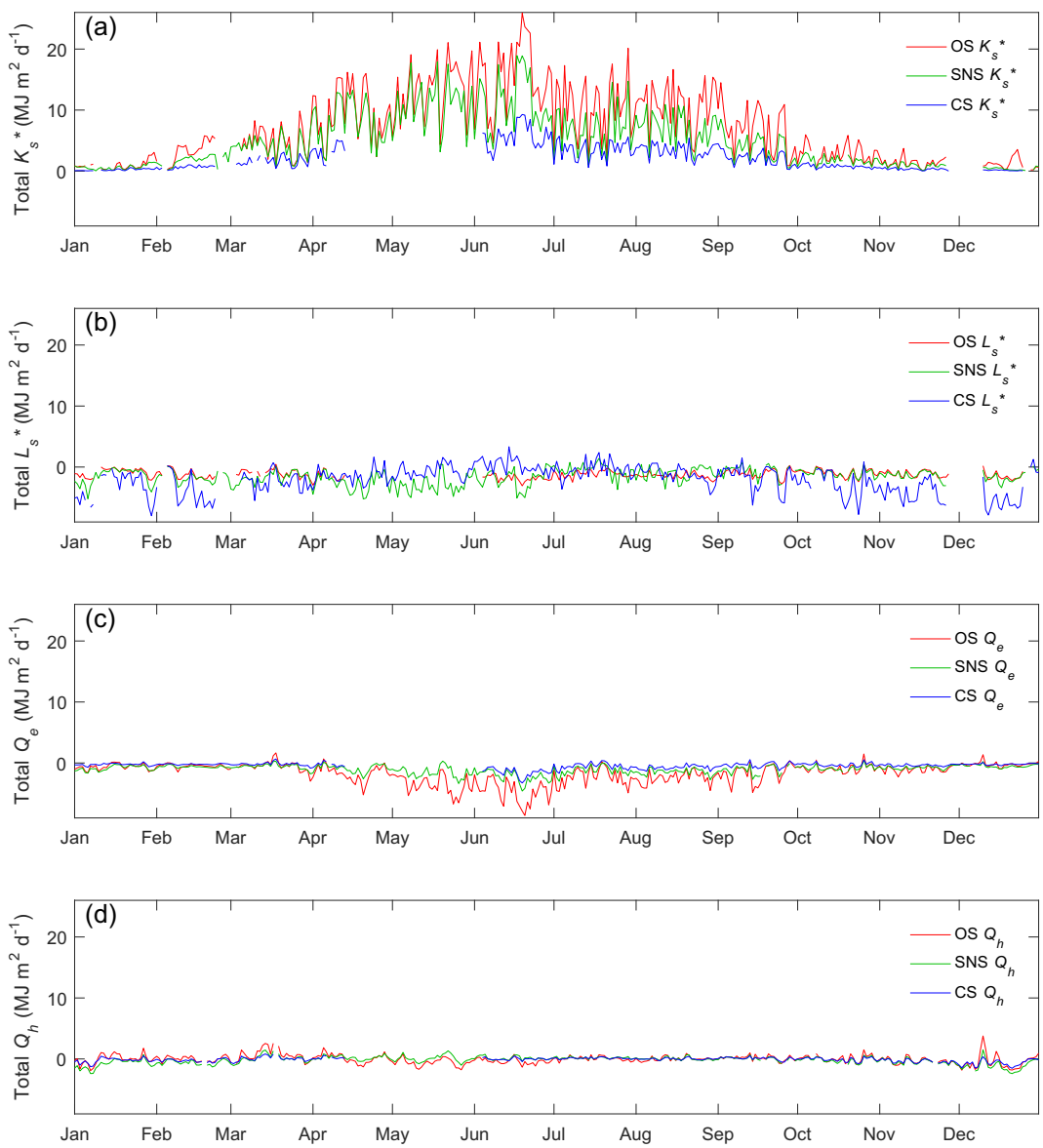

Fig. 3. Daily total net solar shortwave radiation (A) net longwave radiation (B) latent heat energy flux (C) and sensible energy flux (D) derived from observations recorded by AWS.

Table 3
Descriptive statistics (daily mean, minimum, maximum and standard deviation) for variables describing energy fluxes at air-water interface.

		Annual				Winter				Summer			
Variable	Site	Mean	Min	Max	SD	Mean	Min	Max	SD	Mean	Min	Max	SD
Q_{sn} (MJ m^2 d^{-1})	OS	2.6	−8.5	18.1	6.1	−2.9	−8.5	4.3	2.9	8.5	−1.7	18.1	4.6
Q_{sn} (MJ m^2 d^{-1})	SNS	1.8	−6.1	12.6	3.9	−2.2	−6.1	1.9	1.9	5.6	−0.3	12.6	2.8
Q_{sn} (MJ m^2 d^{-1})	CS	0.3	−3.8	5.6	1.8	−1.4	−3.8	0.9	1.2	1.9	−0.1	5.6	1.2
Q^* (MJ m^2 d^{-1})	OS	4.1	−6.4	24.7	7.1	−2.3	−6.4	2.3	2.1	11.7	0.2	24.7	5.9
Q^* (MJ m^2 d^{-1})	SNS	2.9	−2.9	14.4	3.9	−0.7	−2.9	1.6	1.0	7.1	0.8	14.4	3.2
Q^* (MJ m^2 d^{-1})	CS	0.8	−2.2	7.1	1.8	−0.8	−2.2	0.7	0.8	2.7	0.1	7.1	1.5
K_s^* (MJ m^2 d^{-1})	OS	6.3	0.1	25.9	5.7	1.8	0.1	5.8	1.6	12.2	1.9	25.9	5.3
K_s^* (MJ m^2 d^{-1})	SNS	4.3	0.1	18.9	4.1	1.0	0.1	2.8	0.8	8.2	1.0	18.9	4.1
K_s^* (MJ m^2 d^{-1})	CS	2.0	0.0	9.3	2.0	0.3	0.0	1.0	0.3	4.1	0.6	9.3	1.9
L_s^* (MJ m^2 d^{-1})	OS	−2.2	−8.0	3.3	2.3	−4.1	−8.0	0.2	2.3	−0.5	−4.6	3.3	1.4
L_s^* (MJ m^2 d^{-1})	SNS	−1.3	−5.1	1.4	1.1	−1.7	−4.1	0.1	1.0	−1.2	−5.1	1.4	1.4
L_s^* (MJ m^2 d^{-1})	CS	−1.2	−3.1	0.4	0.7	−1.1	−2.2	0.2	0.7	−1.4	−3.1	−0.2	0.6
Q_e (MJ m^2 d^{-1})	OS	−1.5	−8.6	1.7	1.6	−0.5	−1.6	1.4	0.5	−3.1	−8.6	0.2	1.8
Q_e (MJ m^2 d^{-1})	SNS	−1.0	−4.6	0.5	0.7	−0.7	−1.7	0.2	0.3	−1.6	−4.6	0.0	0.9
Q_e (MJ m^2 d^{-1})	CS	−0.4	−3.3	0.7	0.5	−0.2	−0.7	0.2	0.1	−0.9	−3.3	0.4	0.7
Q_h (MJ m^2 d^{-1})	OS	0.0	−1.9	3.8	0.8	−0.2	−1.9	3.8	1.0	−0.1	−1.4	0.9	0.4
Q_h (MJ m^2 d^{-1})	SNS	−0.2	−2.4	1.5	0.7	−0.8	−2.4	1.5	0.7	0.1	−0.4	0.8	0.3
Q_h (MJ m^2 d^{-1})	CS	−0.1	−1.5	0.8	0.4	−0.4	−1.5	0.5	0.5	0.1	−0.4	0.5	0.2

1 MJ m^2 d^{-1}) during October to February but more pronounced during the remaining part of the year.

Averaged over the course of the year, SNS and CS lose energy due to sensible heat exchange (−0.2 ± 0.7 and −0.1 ± 0.4 MJ m^2 d^{-1} respectively) while Q_h at OS contributed an almost negligible amount to the overall energy budget (0.0 ± 0.8 MJ m^2 d^{-1}). While the differences between the three sites were not found to be significant, there is some (albeit limited) evidence for inter-site variability in annual trends (Fig. 3d), presumably (like Q_e) due to differences in humidity and wind speed. At OS, Q_h is generally stationary with little seasonal change in mean. However, standard deviation is decreased in summer compared to winter (1.0 vs 0.4 MJ m^2 d^{-1}; Table 3), indicating that the magnitude of daily Q_h fluctuations have a strong seasonal component. In addition to this seasonal variability in the magnitude of daily Q_h fluctuations, SNS and CS also display a non-stationary trend whereby energy is lost due to sensible heat flux in the winter and gained during summer (−0.8 vs −0.1 and 0.1 vs 0.1 MJ m^2 d^{-1} for SNS and CS respectively).

3.3. Energy fluxes at the water-streambed interface

Total heat flux (Q_{bhf}) between the channel and streambed is several orders of magnitude lower than at the air-water interface (Table 4). While no significant difference was observed in the mean streambed heat flux recorded across the three sites, seasonal patterns vary between sites (Fig. 4a). OS recorded both the highest (mean) and most variable bed heat flux (0.1 ± 0.6 MJ m^2 d^{-1}) and also exhibited a moderate seasonal trend whereby the streambed generally acts as a heat source in winter ($\bar{x}$ = 0.5 MJ m^2 d^{-1}) and sink during summer ($\bar{x}$ = −0.6 MJ m^2 d^{-1}). At CS, despite the considerable loss of data, available records suggest the existence of broadly similar seasonal trends to OS ($\bar{x}$ = 0.1 and −0.3 MJ m^2 d^{-1} for winter and summer respectively). However, averaged across the year, mean bed heat flux is negative and temporal variability is muted (−0.1 ± 0.3 MJ m^2 d^{-1}) in comparison to OS, indicating that bed heat fluxes contribute less to river temperature. Bed heat flux at SNS is more clearly different to OS or CS. Although mean Q_{bhf} at SNS was situated between the other two sites (0.0 MJ m^2 d^{-1}), daily variability was substantially reduced (σ = 0.1 MJ m^2 d^{-1}). Furthermore, although cursory inspection of the data suggests that like OS/CS, bed heat flux is negative in summer and positive in winter ($\bar{x}$ = 0.1 and −0.1 MJ m^2 d^{-1} respectively), the magnitude of bed heat fluxes is extremely small.

Net radiative fluxes at the streambed follow broadly similar trends to those at the air-water interface. However, none of the inter-site differences in Q_b^* (and also K_b^* and L_b^*) were found to be significant. In terms of annual cycling in net solar radiation received by the bed, maximum K_b^* values were observed near to the summer solstice and extremely low values (<0.5 MJ m^2 d^{-1}) were recorded at all sites during the winter months (Fig. 4b). These winter minima result in

Table 4
Descriptive statistics (daily mean, minimum, maximum and standard deviation) for variables describing energy fluxes at streambed interface.

		Annual				Winter				Summer			
Variable	Site	Mean	Min	Max	SD	Mean	Min	Max	SD	Mean	Min	Max	SD
Q_{bhf} (MJ m^2 d^{-1})	OS	0.1	−2.1	1.4	0.6	0.5	−0.4	1.4	0.3	−0.6	−2.1	0.9	0.6
Q_{bhf} (MJ m^2 d^{-1})	SNS	0.0	−0.4	0.5	0.1	0.1	0.0	0.2	0.0	−0.1	−0.4	0.2	0.1
Q_{bhf} (MJ m^2 d^{-1})	CS	−0.1	−1.5	0.8	0.3	0.1	−0.1	0.3	0.1	−0.3	−1.5	0.4	0.4
Q_b^* (MJ m^2 d^{-1})	OS	2.6	−0.2	8.7	2.4	–	–	–	–	4.2	0.5	8.7	2.2
Q_b^* (MJ m^2 d^{-1})	SNS	1.9	0.0	6.2	1.8	–	–	–	–	3.2	0.1	6.2	1.6
Q_b^* (MJ m^2 d^{-1})	CS	1.8	−0.4	6.7	1.9	–	–	–	–	3.1	0.4	6.7	1.8
K_b^* (MJ m^2 d^{-1})	OS	1.6	0.0	8.3	1.9	0.4	0.0	0.7	0.2	3.9	0.7	8.3	2.0
K_b^* (MJ m^2 d^{-1})	SNS	1.3	0.0	6.1	1.4	0.5	0.1	1.1	0.2	3.1	0.2	6.1	1.5
K_b^* (MJ m^2 d^{-1})	CS	1.2	0.0	6.5	1.4	0.3	0.0	0.8	0.2	2.9	0.5	6.5	1.7
L_b^* (MJ m^2 d^{-1})	OS	−0.1	−0.7	1.0	0.3	−0.3	−0.5	−0.1	0.1	0.1	−0.5	1.0	0.3
L_b^* (MJ m^2 d^{-1})	SNS	0.0	−0.2	0.2	0.1	0.0	−0.2	0.1	0.1	0.0	−0.2	0.2	0.1
L_b^* (MJ m^2 d^{-1})	CS	−0.1	−0.5	0.4	0.1	−0.2	−0.3	−0.1	0.1	0.0	−0.3	0.4	0.1

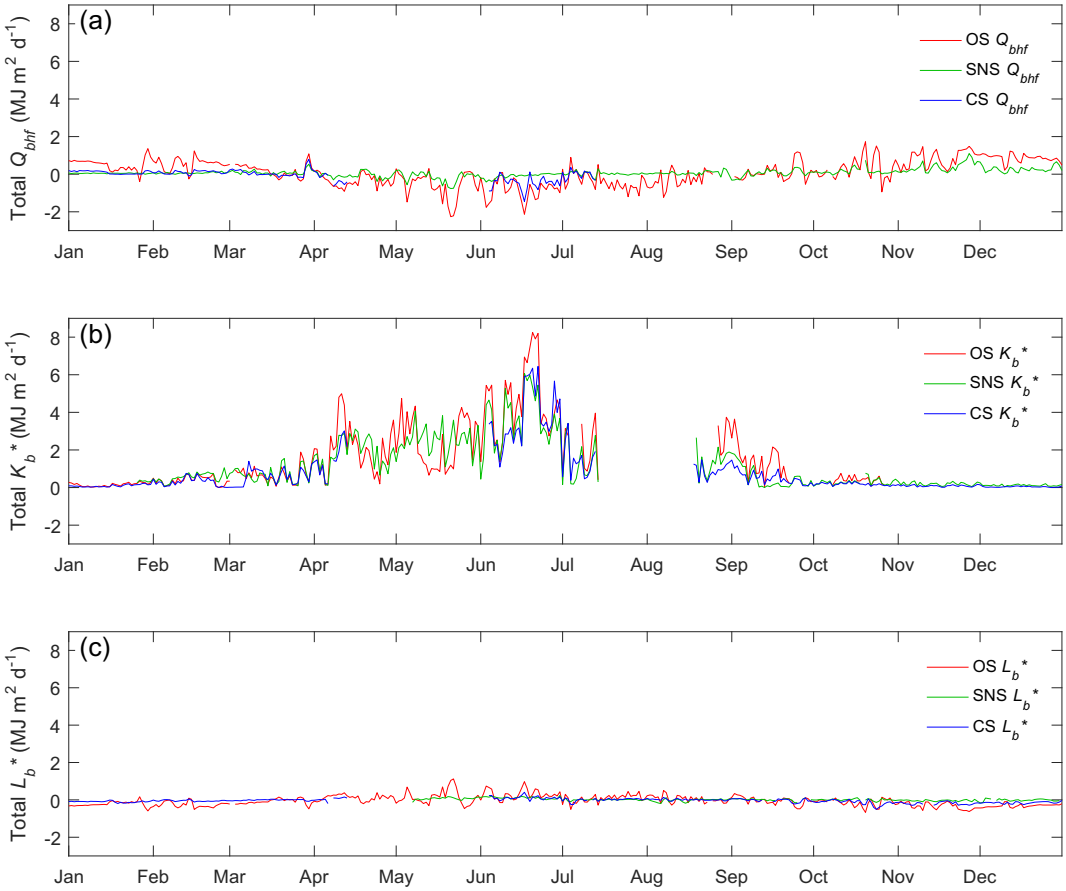

Fig. 4. Daily total bed heat flux (A) net solar shortwave radiation (B) and net longwave radiation (C) derived from observations recorded by AWS. Note that zero-values for K_b* during winter months are not erroneous and in fact represent occasions where winter ice/snow cover prevented radiation from reaching pyranometer.

part from persistent ice cover which blocked incoming solar radiation at the stream surface. In terms of seasonal patterns in longwave radiation, OS is characterised by a relatively strong annual cycle, with positive L_b* values mainly recorded during the summer months and negative values in the winter (Fig. 4c). CS demonstrates a similar annual trend, but with a lower range. Calculation of L_b* for SNS was limited to periods where streambed temperature data at 0.05 m was available (Fig. S2), meaning that it is difficult to discern any clear annual/seasonal cycle.

3.4. Total energy available

Owing to the relatively minor contribution of bed heat flux to the overall energy balance and the large loss of bed heat flux measurements at CS, comparison of the total energy available at each site is given in terms of total heat flux at the water surface (Q_{sn}; Fig. 5a) rather than total heat flux (Q_n). Averaged over the course of the year, all three reaches revealed a net energy gain (Table 3). However, the magnitude of energy fluxes differs significantly ($p < 0.01$) between the three sites, with OS recording the highest gain (2.6 MJ m^2 d^{-1}) followed by SNS (1.9 MJ m^2 d^{-1}) and CS (0.3 MJ m^2 d^{-1}). In terms of seasonal variability in net energy available at the stream surface, Q_{sn} is strongly positive in summer ($\bar{x} = 8.5$, 5.6 and 1.9 MJ m^2 d^{-1} respectively), and negative in winter ($\bar{x} = -2.9$, -2.2 and -1.4 MJ m^2 d^{-1} respectively). This result reveals the existence of a clear inversion in site ordering, whereby total energy fluxes are ordered OS > SNS > CS in summer and CS > SNS > OS in winter. Although missing data means that it is difficult to determine exactly where this transition occurs, inspection of Fig. 5a indicates that inter-site differences in net energy fluxes are minimised during mid-March and mid-October. It is therefore likely that the vernal and autumnal equinoxes mark the transition from winter to summer energy balance. Regression analysis allows for the quantification of the inter-site similarity between energy fluxes. These data permit a further understanding into how each site 'behaves' from an energy balance point of view. At first glance, Table 5 appears to shows slightly conflicting results in terms of inter-site similarity between the various fluxes. Turbulent (Q_e and Q_h) and longwave exchanges indicate that the SNS-CS correlation is generally highest, whereas in terms of solar radiation, the correlation is maximised between OS and SNS. However, given the relative contribution of K_s* to the overall energy balance, this has the effect of yielding a clear distinction in terms of total energy flux (Q_{sn}), whereby the high degree of correlation between OS and SNS indicates that these sites are much more closely matched in terms of energy balance than either OS/CS or SNS/CS.

Table 6 highlights seasonal variability in the relative contribution of different heat sources/sinks to the energy balance at each site. In terms of energy gains, K_s* is the dominant heat source across all seasons (Fig. 5b–d). However, its relative contribution to the energy balance is lowest in the winter, where Q_h contributes the bulk of the remaining positive energy budget (Table 6). This effect is greatest at OS (and to a lesser extent, CS), where freeze-up conditions drive Q_h gain; the higher winter water temperatures at SNS explain the lower Q_h contribution at this site. In summer, Q_h is a relatively minor contributor to energy gains, but is higher at CS and SNS than OS. Latent heat (Q_e) gains also contribute more to the winter energy balance than in summer, particularly at OS and CS, (presumably due to condensation on ice cover at these sites). In terms of longwave radiation, L_s* is a minor contributor to energy gains at CS during the winter, but is negligible at OS or SNS. However, this pattern inverts in the summer, with L_s* contributing nothing to energy gains at CS, but a small amount at SNS and OS.

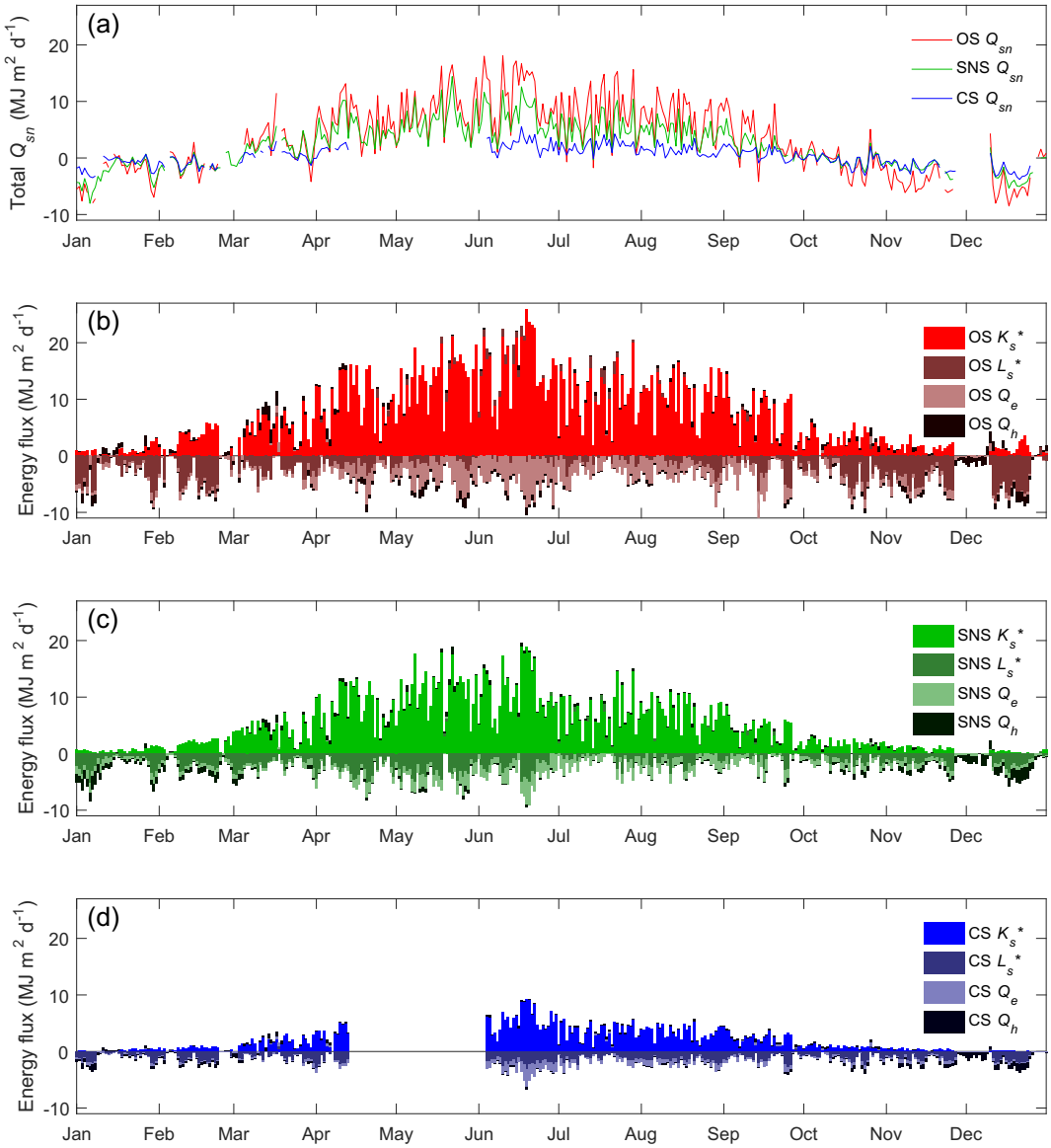

Fig. 5. (A) Daily total energy flux at air-water interface derived from observations recorded by AWS. (B)–(D) Partitioning of energy flux at air-water interface at (B) OS (open grassland), (C) SNS (semi-natural woodland) and (D) CS (commercial coniferous woodland), allowing for visualisation of stream temperature maxima/minima.

L_s* is the dominant heat sink when averaged over the course of the year, followed by Q_e and Q_h. However, closer inspection of the seasonal components reveals considerable sub-annual and inter-site variability in heat loss partitioning. In the winter, L_s* is the dominant heat sink at all sites. However, while L_s* is responsible for over three-quarters of energy losses at OS, its contribution is much reduced at CS and especially SNS. In the summer, L_s* remains the dominant heat sink at CS (accounting for two-thirds of energy losses), but is a substantially smaller term at OS and SNS where it is superseded by Q_e as the dominant heat loss term. Indeed, latent energy exchanges contribute substantially to summer losses at all sites, particularly at Q_e. In the winter, Q_e-driven losses display an inverted pattern, with SNS recording the highest magnitude loss, presumably due to the increased winter stream temperature at SNS. Remaining energy transfers away from the stream are driven by sensible heat processes, the magnitude of which changes considerably between winter and summer. In winter, Q_h is a substantial heat loss term at SNS, again presumably due to elevated winter stream temperatures at this site. Q_h is slightly lower at CS and more substantially reduced at OS, but still represents a notable heat sink at all sites. However, in summer, Q_h contributes extremely little to heat loss at SNS and CS, and while greater at OS, is still a relatively heat sink term.

Table 5
Correlation Table showing coefficient of determination (R^2) between energy fluxes at air-water interface recorded at OS and SNS, OS and CS and SNS and CS. Values can be considered a measure of 'similarity' between sites in terms of their energy fluxes. All R^2 values are significant ($p < 0.01$).

	Qsn	Ks*	Ls*	Qe	Qh
OS, SNS	0.83	0.84	0.14	0.77	0.74
OS, CS	0.57	0.75	0.32	0.78	0.72
SNS, CS	0.54	0.81	0.32	0.82	0.74

4. Discussion

4.1. Stream temperature and energy flux response to different forest cover

This study extends the findings of existing investigations into the effects of riparian woodland on river energy budgets and temperature regimes. While the majority of previous studies focused on comparing

Table 6
Partitioning of energy fluxes at air-water interface. All data given in %. Variables marked with '+' denote energy gains; '−' denotes energy losses.

	Variable	OS	SNS	CS
Total	K_s^*+	93.5	96.1	94.6
	L_s^*+	1.9	0.8	0.2
	Q_e+	0.4	0.1	0.9
	Q_h+	4.2	3.0	4.3
	K_s^*-	0.0	0.0	0.0
	L_s^*-	56.0	49.6	64.5
	Q_e-	38.3	38.7	26.4
	Q_h-	5.7	11.7	9.1
Winter	K_s^*+	83.3	95.6	87.5
	L_s^*+	0.2	0.2	2.3
	Q_e+	1.8	0.4	1.3
	Q_h+	14.7	3.8	8.8
	K_s^*-	0.0	0.0	0.0
	L_s^*-	81.1	51.3	64.1
	Q_e-	10.4	21.5	13.1
	Q_h-	8.5	27.3	22.8
Summer	K_s^*+	96.2	97.2	97.5
	L_s^*+	2.8	1.0	0.0
	Q_e+	0.0	0.0	0.3
	Q_h+	0.9	1.8	2.2
	K_s^*-	0.0	0.0	0.0
	L_s^*-	20.3	42.7	60.4
	Q_e-	74.4	55.5	37.8
	Q_h-	5.3	1.8	1.8

forested environments to open moorland/grassland/clearcut, here we provide an insight into how river temperatures and corresponding heat fluxes are dependent upon the specific type of forest cover. The results of this study provide new information to help refine understanding of river temperatures under contrasting land uses, and have important implications for forest and river management practises in temperate regions (in which these forest types are endemic). This study agrees with previous research (e.g. Broadmeadow et al., 2011; Hannah et al., 2008; Webb and Zhang, 2004) which indicates that deciduous forest cover (SNS) is able to moderate summer stream temperatures in a similar fashion to (potentially denser) conifer forest (CS). However, in this investigation, summer stream temperatures at SNS were found to be significantly warmer than at CS. Indeed, while mean summer stream temperature at CS was 1.0 °C cooler than OS, this difference was halved at SNS ($\Delta\bar{T}_w$(SNS,OS) = 0.5 °C). Inspection of energy budget data assembled from the AWS observations at each site outlines the reasons for these results.

During the summer months, net surface heat flux (Q_{sn}) was ordered OS > SNS > CS. Because surface heat flux (Q_{sn}) is a major (generally, *the* major; Hannah et al., 2008; Webb and Zhang, 1997, 1999) driver of summer stream temperatures, it is unsurprising that summer T_w followed this same order. Solar radiation is the principal mechanism controlling surface heat flux in summer (Caissie, 2006). These inter-site variations in surface heat flux (and, by extension, water temperature) therefore arise from significant differences in solar radiation received at the stream surface. K_s^* variability between the three sites is driven by changes in the cover of riparian woodland at each site. This forest cover acts to shade the stream from K_s^*, effectively blocking a given proportion of solar radiation from being received at the stream surface. CS recorded the smallest energy gain due to the presence of dense conifer vegetation which blocked K_s^*, limiting the amount of energy received at the air-water interface. The dense forest also reduced wind speeds and augmented humidity in relation to OS and SNS, thus limiting turbulent heat exchange. Nevertheless, the reduction in Q_e losses that this entailed (in comparison to OS) was not sufficient to supplant the shortfall in net energy produced by the reduction in K_s^*. Conversely, OS recorded the highest net energy gain (and hence, highest stream temperature) due to the absence of any riparian vegetation that would otherwise block solar radiation received at the stream surface. Although this, combined with increased wind speed due to the absence of tree cover, drove significantly higher latent heat fluxes at OS in comparison to SNS or CS, the magnitude of these exchanges was insufficient to offset the effect of the increased K_s^* values on water temperature. At SNS, summer energy gain at the air-stream interface was a composite of that of CS and OS. Like CS, K_s^* was reduced in comparison to OS due to the presence of forest cover. However, a significantly larger amount of solar radiation was received at the air-water interface than at CS. This increase in K_s^* indicates that in this study, deciduous vegetation provided a lower degree of shading than the coniferous cover.

While previous studies have indicated that light transmission is normally lower through deciduous trees than through coniferous vegetation (e.g. Konarska et al., 2014; Lintunen et al., 2013), this investigation recorded significantly higher K_s^* at SNS than at CS. This apparent contradiction is presumably due to the fact that forest cover at SNS was much lower than at CS. Hemispheric photography of the riparian canopy at SNS and CS supports this theory, whereby forest cover at CS (quantified here using Gap Light Analyzer; Frazer et al., 1999 as the proportion of light in the above-stream hemisphere that is blocked by vegetation; see Garner et al., 2014) was found to be substantially higher than at SNS (80% vs 66%). This lower forest cover relative to CS also explains why wind speed and humidity were reduced (and hence, evaporative heat losses increased) in comparison to the conifer site. Taken together, and given the lack of significant inter-site differences between any of the other energy budget terms recorded in this investigation (e.g. longwave radiation, sensible heat flux), these results clearly demonstrate that summer stream temperature differences between forest treatments are driven by inter-site variability in K_s^* resulting from differing levels of riparian shading (rather than by variability in the other components of the stream energy budget). Furthermore, our findings suggest that while both deciduous and coniferous forest types are able to moderate summer water temperatures, their effectiveness in doing so differs significantly, likely as a function of their contrasting stand densities (i.e. no. of trees per m^2), forest structure (e.g. shape and size of the canopy and branches; Lim et al., 2003) and canopy architecture (e.g. leaf area index and leaf inclination; Welles et al., 1991).

The long-term perspective offered by this dataset also allows for an insight into how winter stream temperatures and energy budgets vary between forest treatments. Substantial differences in winter stream temperature were observed between the three sites, and it is pertinent to examine the extent to which this variability was driven by the effects of forest cover on radiative energy transfers. Solar radiation (K_s^*) followed the same trends as during the summer, with lowest values recorded at CS and highest values at OS. While this trend again emphasises the role of forest cover in preventing solar radiation from reaching the stream surface, the picture is slightly more complex in winter. During these colder months, net radiation (Q^*) was ordered CS > SNS > OS because the presence of riparian canopy at CS (and to a lesser extent, bare tree limbs at SNS) acted to limit radiative losses by retaining and re-emitting longwave energy towards the stream surface. Given the magnitude of these L_s^* fluxes, net surface heat flux (Q_{sn}) was also consequently ordered CS > SNS > OS. However, stream temperatures did not mirror this result, with SNS instead recording substantially (significantly) higher temperatures than CS or OS. This departure from the expected pattern warrants detailed investigation. It is likely that these anomalously warm temperatures are due to groundwater exfiltration, but the lack of significant differences in bed heat flux between the three sites (or bed temperature data indicative of cool groundwater inflows at SNS during summer) means that any groundwater inputs into the SNS reach must occur upstream of the AWS. The increased winter stream temperatures recorded at SNS are therefore most plausibly due to heat advected from warm groundwater inputs upstream of the study reach. Energy advected towards SNS also accounts for the increased losses from sensible and latent heat during the winter because of the increased air-water temperature gradient in comparison to CS or OS. Overall, this apparently contradictory result at SNS has important

implications for understanding the effects of forest cover on stream temperature and energy fluxes. In winter, the lower magnitude of net radiation (when compared to the summer) means that advective processes can have a larger impact on stream temperature than radiative energy transfers. However, in the summer, the substantial increase in radiative energy means that its effect on stream temperatures (and thus, the relative impact of forest cover) is considerably elevated in comparison to other energy fluxes. These results give credence to the findings of Garner et al. (2014) which also emphasise the importance of considering the influence of advective heat on stream temperatures, in addition to radiative fluxes.

While it might be expected a priori that energy fluxes at SNS and CS behave similarly (given the presence of riparian vegetation at both sites and the implications of this energy flux variability), regression analysis suggests that this was not necessarily the case. Instead, OS and SNS were found to be more closely correlated in terms of net surface heat flux (Table 5). This result is presumably a function of both a) the increased transmission of K_s^* at SNS during the summer (in comparison to CS), b) the relative similarity of energy fluxes at OS and SNS during the winter, owing to the lack of foliage at SNS. Furthermore, the grid-like commercial plantation layout at CS results in an uneven diel shortwave flux cycle, whereby unlike at SNS (where shortwave radiation is uniformly reduced throughout the day), solar radiation at CS is substantially reduced by the dense forest stand until the sun reaches its zenith (midday), at which point there is sufficient space between individual trees for solar radiation to strike the water surface almost unimpeded. These potentially unexpected findings further highlight the fact that that the impacts of forest cover on river energy budgets are not fixed, and that the interaction between K_s^* and riparian forests varies across multiple axes of forest structure, canopy architecture and stand density.

4.2. Comparisons with other studies

4.2.1. Impacts of riparian vegetation on stream temperature.

In broad terms, the results of this study agree with other literature that demonstrates stream temperature reductions under forest cover when compared to open terrain (e.g. Brown et al., 2010; Hannah et al., 2008; Malcolm et al., 2008; Moore et al., 2005a; Webb and Crisp, 2006). However, detailed inter-comparison of the results of this study with similar investigations is difficult. Although a large amount of literature exists comparing stream temperatures and energy fluxes under (predominantly conifer) forested and open terrain, complications arise from a) their use of varying temperature metrics, b) the bias towards limited-length study periods that only encompass summer data (Malcolm et al., 2008) and c) the high degree of geographic variability among studies which encompass locations as disparate as New Zealand (e.g. Rowe et al., 1994), western Canada (e.g. Moore et al., 2005b) and the south-west United Kingdom (e.g. Webb and Zhang, 2004).

The vast majority of previous studies (particularly in the pre-2005 literature) comparing stream temperatures under forested and open terrain derive from the West Coast of North America (see Caissie, 2006; Moore et al., 2005a for review). Most of these studies only comprise summer data, and generally examine differences in maximum recorded temperature between conifer-lined reaches and agroforestry clear-cuts. Although some recent studies report relatively small differences in summer maximum temperature between forested and open terrain in the Pacific Northwest (~1–2 °C; Guenther et al., 2014; Janisch et al., 2012; Kibler et al., 2013; Pollock et al., 2009), differences in maximum summer temperatures on the order of 4–9 °C are more common (e.g. Dunham et al., 2007; Kreutzweiser et al., 2009; Leach et al., 2012; Moore et al., 2005a). Indeed, increases in summer maximums of up to 13 °C have occasionally been recorded following clearcutting of commercial conifer plantations (Moore et al., 2005a). In this study, the largest daily difference in summer maximum temperature between CS and OS were towards the lower end of this scale ($\Delta T_{w,\max}$(OS,CS) = 3.9 °C), presumably due to the fact that that a substantial upstream area of the OS catchment is forested and water entering the study reach was already reasonably cool. This may explain the reduced temperature difference in comparison to studies from North America where clearcutting covers much larger areas, but the considerable differences in latitude, prevailing hydroclimatic conditions and catchment hydromorphology between our study site (west coast of Scotland) and the Pacific Northwest of North America mean that limited inferences can be drawn from this result.

Instead, it is more relevant to compare this study to previous investigations conducted in the United Kingdom, minimising differences arising from hydroclimatology and hydromorphology. Many previous studies from the UK incorporate longer term datasets (e.g. Garner et al., 2015; Hannah et al., 2008; Webb and Zhang, 2004) than those from other regions, providing additional information about stream temperature response to forest conditions during different seasons. Furthermore, rather than focusing solely on coniferous forest types, several UK-based studies have also examined stream temperature responses to deciduous vegetation, meaning that a fuller comparison of the results of this investigation can be achieved. These studies often record temperatures in terms of daily (or seasonal) means rather than maximums, further facilitating comparison with this investigation. In terms of mean annual temperature differences between forest treatments, Hannah et al. (2008) reported that stream temperature was 0.14 °C warmer in deciduous woodland than in open moorland. However, studies examining annual temperature patterns between conifer-covered reaches and open terrain reported opposite trends, with forested reaches 0.4–0.9 °C cooler than open/clear-cut sites (Brown et al., 2010; Stott and Marks, 2000; Crisp, 1997; Webb and Crisp, 2006). While the results of this study demonstrate similar trends (deciduous site warmer and conifer site cooler than open site), the magnitude of differences between OS and SNS (−0.8 °C) was considerably higher than that reported by Hannah et al. (2008), presumably because of the (postulated) winter advective flux at SNS. However, the mean annual difference between OS and CS (+0.3 °C) was closer to that recorded by previous studies examining the effects of coniferous cover (e.g. Crisp, 1997; Stott and Marks, 2000; Webb and Crisp, 2006).

In terms of mean summer temperatures, previous studies report differences of 2–3 °C between conifer and open reaches (e.g. Brown et al., 2010; Webb and Crisp, 2006), whereas differences between deciduous and open reaches are generally on the order of 1–2 °C (e.g. Broadmeadow et al., 2011; Garner et al., 2015; Hannah et al., 2008; Imholt et al., 2010; Malcolm et al., 2004; Malcolm et al., 2008). Although summer mean differences reported in this study are approximately half of these values for both the conifer and deciduous forest treatments (1.0 and 0.5 °C respectively), they follow the same general trend of deciduous woodland moderating summer temperatures to a lesser extent than coniferous forest. The lower values presumably result from a combination of factors including differences in basin hydromorphology and geology, but are also likely due in part to the fact that Loch Ard is situated on the west coast of Scotland, where maritime conditions provide a different hydroclimatic context to previous UK-based studies (e.g. Broadmeadow et al., 2011; Brown et al., 2010; Hannah et al., 2008).

4.2.2. Impacts of riparian vegetation on energy budgets and radiative fluxes.

Energy budget partitioning in this study is generally consistent with similar studies that also highlight net radiation as a dominant source of energy at the air-water interface (Caissie, 2006; Evans et al., 1998; Hannah et al., 2008; Leach and Moore, 2010; Webb and Zhang, 1997, 1999, 2004). However, while an inter-comparison of the relative magnitude of net or solar radiation received under different forest treatments would be useful, there remain very few similar paired-site investigations to which the findings of this study can be contrasted. However, in one notable example, Hannah et al. (2008) observed that over the course of the year, a stream running through deciduous forest received approximately 41% of the solar radiation of the open (moorland) site.

Meta-analysis of similar data from Broadmeadow et al. (2011) indicates that mixed deciduous and coniferous woodland received an average of 33% of the radiation of open terrain. Both of these reductions are considerably higher than that recorded in this study, which indicates SNS received ~67% of the mean annual solar radiation of OS. However, the difference in K_s* received between CS and OS (32%) is broadly similar to that reported by Broadmeadow et al. (2011).

Inconsistencies in the reduction of solar radiation under deciduous forest cover between this study and previous research again likely results from differences in the forest environment present. Indeed, Webb and Zhang (1997) highlight the fact that the effect of tree cover on solar radiation attenuation can be highly variable. An examination of the absolute magnitude of energy fluxes recorded in this study reveals potential reasons for the lower-than-expected temperature reductions under forest treatments (when compared to other studies). Although it would be fallacious to compare absolute energy flux values between studies conducted at substantially different locations, Hannah et al. (2008) was conducted at a broadly similar latitude. A comparison of annual mean values between Loch Ard and the Girnock Burn (Cairngorms National Park, Scotland) site detailed in Hannah et al. (2008) is therefore relatively valid. Comparing OS to a similarly open site at Girnock Burn, there was little difference in the mean annual K_s* observed (6.3 vs. 6.3 MJ m^2 d^{-1} respectively). However, L_s* and Q_e losses observed by Hannah et al. (2008) were indeed greater than in this study (−2.2 vs −3.9 for L_s* and −1.5 vs −2.3 for Q_e at Loch Ard and Girnock Burn respectively). The lower Q_e losses reported here are presumably due to the decreased wind speed observed in this study in comparison to Hannah et al. (2008; 1.0 vs. 2.3 ms^{-1}), while the lower magnitude L_s* loss is partially attributable to the cloudier maritime conditions at Loch Ard. The considerably increased annual precipitation at Loch Ard (approximately 4× that of Girnock Burn) is also likely to have reduced L_s* and Q_e due to increased input from cool runoff. Conversely, when comparing energy fluxes at SNS to an analogous deciduous site at Girnock Burn, K_s* was substantially higher in this study (4.3 vs 2.6 MJ m^2 d^{-1} respectively), while all other fluxes were relatively similar. This increased solar radiation at SNS compared to Hannah et al. (2008) clearly explains why the stream temperature reduction at SNS was lower than previous studies. Indeed, inspection of the results shows that in Loch Ard, it is actually CS (coniferous woodland) that most closely resembles the deciduous woodland reported in Hannah et al. (2008) in terms of energy fluxes. These results explain why the summer stream temperature difference between CS and OS was closer to that reported by Hannah et al. (2008) for deciduous woodland (~1 °C). Indeed, Imholt et al. (2013) note similar occurrences, whereby deciduous woodland in Girnock Burn had a larger impact on stream temperatures than conifer woodland at another nearby location. They attributed the differences to variability in stem density and tree coverage between the two sites. These results therefore lend further credence to the fact that the moderating effect of forest cover on water temperature is not solely a function of forest type or species but the result of a combination of factors including stand density and canopy architecture.

4.3. Implications for river management and future research

The results of this study shed further light on the role of riparian woodland in moderating temperature extremes in river environments. As such, they have important implications for the management of streams and riparian woodlands in order to limit the exposure of aquatic species to summer temperature extremes. Although this study echoes similar previous investigations that clearly highlight the ability of riparian forest to moderate high stream temperatures, the clear difference in stream temperature and energy budget between different forest treatments raises new questions regarding the efficacy of particular forest types and configurations in moderating summer temperature extremes.

While current riparian tree-planting initiatives often consider species or forest type (i.e. coniferous, deciduous) as a factor when determining planting strategies, emphasis is usually placed on the selection of forest types that satisfy anthropogenic demands (e.g. the preferences of landowners and farmers; Lawrence and Dandy, 2014), contribute to the re-establishment of native species (e.g. EA, 2011; Lowe et al., 2012) or conform to arboricultural practicalities (i.e. tree type is governed by what will grow well in a specific environment; Withrow-Robinson et al., 2011). These compromises mean that the resultant forest configuration may indeed be sub-optimal for the generation of shade suitable for moderating stream temperatures. While previous research (e.g. Broadmeadow and Nisbet, 2004) has documented strategies for successfully negotiating these regulatory and scientific requirements when designing effective riparian buffer strips, the goal of such work is often the enhancement of bank stability or the increased input of nutrients to the stream, rather than the specific creation of shading. As a result, Orr et al. (2015) highlight the clear need for more information into the combinations of tree size and buffer spacing that are most effective in generating shade to moderate water temperature, a research gap that recent studies (e.g. Garner et al., 2017) are slowly starting to address.

Given this pressing research need, and in light of the results of this study, we advocate the development of numerical models that are able to simulate tree shading (and the resulting stream temperature response through appropriate energy budget parameterisation) under different combinations of tree species, stand density and canopy architecture. Although many deterministic stream temperature models contain routines that are currently capable of simulating the impacts of tree shading on stream temperature patterns (e.g. Bartholow, 1989; Boyd and Kasper, 2003; Chen et al., 1998), none of the currently-available models are able to differentiate between the subtleties of different forest types or configurations. Furthermore, while an investigation by Imholt et al. (2013) revealed clear statistical linkages between forest allometric features and river temperature patterns, the study was largely empirical in nature and did not consider the effects of forest configuration on radiative transfers. As such, the next generation of stream temperature models should aim to incorporate ray tracing or radiosity approaches common to computer vision or remote sensing (e.g. Bittner et al., 2012; García-Haro et al., 1999; Jones and Vaughan, 2011) in order to more accurately simulate radiative transfers through specific riparian vegetation types and forest structures. The outputs of such models would allowing river managers to optimise riparian plantation strategies in order to maximise summer stream temperature reductions.

Recent research by Garner et al. (2017) simulating stream temperature responses to varying amounts of riparian shading, channel orientations and flow velocities represents a step in the right direction, and illustrates the utility of deterministic models for quantifying the riparian shading configurations that will have the largest water temperature 'impact'. However, there remains considerable uncertainty about how best to upscale the non-radiative energy fluxes recorded at spatially-isolated weather stations to the quasi-continuous streamwise data required by river temperature models. While simulations of shading and or channel orientation can be used to scale radiative energy fluxes from isolated locations to whole-river extents, there are currently no deterministic models that compute the spatially-explicit impacts of riparian vegetation on latent or sensible heat exchange (through changes to wind speed or relative humidity). Although (as seen here), these energy flux components represent a smaller part of a river's overall energy budget and therefore contribute a smaller amount to stream temperature processes, future deterministic models should also look to simulate the impacts of riparian vegetation on these non-radiation energy fluxes. One possible way in which this could be achieved is through the development of empirical coefficients that could be applied to the latent/sensible heat flux components in a similar way to the 'shading factor' currently used to scale shortwave radiation; data necessary for informing these empirical coefficients could be derived from experiments using portable weather stations stationed throughout a variety of different riparian forest types.

In addition to the development of models capable of optimising riparian shading solutions for moderating stream temperatures, future research must also address the secondary impacts of riparian forest plantations on stream ecosystems. In addition to providing shade, riparian vegetation can (for example) modify sediment erosion/deposition regimes (e.g. Broadmeadow and Nisbet, 2004), impact invertebrate communities (both negatively; Rouquette and Thompson, 2005 and positively; Rios and Bailey, 2006) and distribution (through acidification pressure; Malcolm et al., 2014), and influence stream water quality and nutrient loading (e.g. Dosskey et al., 2010; Hefting et al., 2005). Indeed, while coniferous vegetation may produce a greater reduction in summer stream temperature than deciduous forest cover, broadleaf vegetation produces higher quality leaf litter (resulting in increased productivity; Broadmeadow and Nisbet, 2004). All aspects of the river's physico-chemical and biological environment must therefore be considered when devising plantation strategies in order to ensure that in searching for optimal shading results, the introduction of riparian vegetation does not actually result in a negative ecosystem response. Any further research into the comparative effects forest cover on stream temperature should therefore aim to take an holistic approach, comparing the simultaneous impacts of different riparian forest treatments on both stream temperature and ecosystem function.

4.4. Measurement uncertainty

We do not believe that measurement uncertainty impacted the findings of this study. Nevertheless, it is necessary to address potential sources of error within the dataset. In addition to instrument uncertainty associated with variables that were measured directly with instrumentation installed at the AWSs (i.e. air/water temperature, wind speed, relative humidity, shortwave and longwave radiation, bed heat flux), a further degree of uncertainty arises from instrument placement. For example, in the case of the pyranometers/net radiometers used to quantify radiative heat flux, small changes in instrument position can produce measurement variability, especially in shaded conditions where light transmission can vary considerably over a small area. Every attempt was therefore made to ensure that pyranometers/net radiometers were placed in a location where light transmission was consistent and representative of the location; we therefore believe that any uncertainty arising from instrument placement will be substantially less than the (considerable) differences recorded between the various sites. Instrument placement may also drive uncertainty in the streambed heat flux data. Numerous articles have documented substantial spatial variability in bed heat flux and bed temperature profiles (e.g. Birkel et al., 2016; Caissie and Luce, 2017; Gariglio et al., 2013; Leach and Moore, 2014), and given that bed heat flux was only measured in one location at each of our study sites, it is possible that the data recorded here does not adequately represent true bed heat flux or temperature. Nevertheless, given that bed heat flux was found to be several orders of magnitude lower than surface exchanges, uncertainty arising from spatial variability in bed heat flux is unlikely to alter the findings of this study.

Another source of uncertainty in the heat flux calculations arises from the use of equations to compute the turbulent (i.e. latent and sensible) heat fluxes. These fluxes are rarely measured directly, and the vast majority of previous studies (e.g. Hannah et al., 2008; Leach and Moore, 2010; Webb and Zhang, 1997) have, like this investigation, derived these fluxes mathematically using semi-empirical or physically-derived equations. Although this means that it is difficult to ascertain the exact uncertainty associated with the computed latent and sensible heat flux values presented here, a comparative study of various heat flux equations (Ouellet et al., 2014) demonstrated that the Dalton-style equations used in this study to estimate turbulent heat flux performed among the best of the mathematic approaches documented in the literature. Although future studies should aim to improve these estimates using real measures of evaporation derived from mini evaporation pans (e.g. Maheu et al., 2014), we believe that the trends in turbulent heat flux data presented within this study are of sufficient accuracy to support our conclusions regarding the relative impacts of tree shading on stream energy budgets.

5. Conclusion

Future climate change is expected to result in raised summer stream temperatures in many temperate river basins, negatively impacting a wide range of fish species. This is likely to have serious consequences both for stream ecosystems and also for communities who benefit from freshwater fisheries. This investigation adds to the growing body of literature demonstrating the efficacy of riparian tree planting for the moderation of these summer water temperatures, and sheds new light on the response of stream temperature (and above-stream energy budgets) to different forest treatments. While related studies (e.g. Garner et al., 2015) note that the effectiveness of riparian planting will vary as a function of both current and future climatic conditions, our results demonstrate that the efficacy of riparian planting is also highly dependent upon the type and structure of forest stands. Future investigations into the effects of climate change on stream temperature must therefore consider not only future climatic/hydrological variability, but must also account for land-use with particular attention paid to the impacts of differing riparian vegetation. Coupled to the increasing sophistication of climate-hydrological-water temperature models, the recent proliferation of monitored riparian planting schemes across the UK and elsewhere means that there is increasing scope to study and analyse the real-world results of riparian planting on stream temperatures. Our results also highlight the complexity of the energy balance response to differing riparian vegetation types, not only in terms of the impact of riparian tree cover on shortwave radiation, but also its influence on all energy fluxes at the air-water interface. Data such as those presented here will be increasingly important for the adequate parameterisation of process-based stream temperature models. However, as data from existing tree-planting schemes becomes increasingly available, it is hoped that it will also be possible to use this to further refine stream temperature models to ensure they are able to fully account for the impacts of different riparian forest types on stream temperature. Such advances will not only add to the growing body of evidence regarding the impacts of climate change on rivers, but will also contribute to efforts to mitigate the effects of such changes on sensitive river environments.

Acknowledgements

This work was supported by a NERC Open CASE studentship (University of Birmingham and Marine Scotland Science) held by KK (grant reference NE/G523963/1). The authors wish to acknowledge the help and support of staff from Marine Scotland Science (Freshwater Fisheries Laboratory) who helped with data collection and storage.

Appendix A. Supplementary data

Supplementary data to this article can be found online at http://dx.doi.org/10.1016/j.scitotenv.2017.08.198.

References

Bartholow, J.M., 1989. Stream temperature investigations: field and analytic methods. Biological Report 89(17). US Fish and Wildlife Service, Washington, D.C.

Benyahya, L., Caissie, D., St-Hilaire, A., Ouarda, T.B.M.J., Bobée, B., 2007. A review of statistical water temperature models. Can. Water Resour. J. 32, 179–192.

Benyahya, L., Caissie, D., Satish, M.G., El-Jabi, N., 2012. Long-wave radiation and heat flux estimates within a small tributary in Catamaran Brook (New Brunswick, Canada). Hydrol. Process. 26, 475–484.

Birkel, C., Soulsby, C., Irvine, D.J., Malcolm, I., Lautz, L.K., Tetzlaff, D., 2016. Heat-based hyporheic flux calculations in heterogeneous salmon spawning gravels. Aquat. Sci. 78, 203–213.

Bittner, S., Gayler, S., Biernath, C., Winkler, J.B., Seifert, S., Pretzsch, H., Priesack, E., 2012. Evaluation of a ray-tracing canopy light model based on terrestrial laser scans. Can. J. Remote. Sens. 38, 619–628.
Bowen, I.S., 1926. The ratio of heat losses by conduction and by evaporation from any water surface. Phys. Rev. 27, 779–787.
Boyd, M., Kasper, B., 2003. Analytical Methods for Dynamic Open Channel Heat and Mass Transfer: Methodology for Heat Source Model Version 7.0. Oregon Department of Environmental Quality, Portland, OR.
Breau, C., Cunjak, R.A., Peake, S.J., 2011. Behaviour during elevated water temperatures: can physiology explain movement of juvenile Atlantic salmon to cool water? J. Anim. Ecol. 80, 844–853.
Broadmeadow, S., Nisbet, T.R., 2004. The effects of riparian forest management on the freshwater environment: a literature review of best management practice. Hydrol. Earth Syst. Sci. 8, 286–305.
Broadmeadow, S.B., Jones, J.G., Langford, T.E.L., Shaw, P.J., Nisbet, T.R., 2011. The influence of riparian shade on lowland stream water temperatures in southern England and their viability for brown trout. River Res. Appl. 27, 226–237.
Brown, G.W., Krygier, J.T., 1970. Effects of clear-cutting on stream temperature. Water Resour. Res. 6, 1133–1139.
Brown, L.E., Cooper, L., Holden, J., Ramchunder, S.J., 2010. A comparison of stream water temperature regimes from open and afforested moorland, Yorkshire Dales, northern England. Hydrol. Process. 24, 3206–3218.
Burton, T.M., Likens, G.E., 1973. The effect of strip-cutting on stream temperatures in the Hubbard Brook Experimental Forest, New Hampshire. Bioscience 23, 433–435.
Caissie, D., 2006. The thermal regime of rivers: a review. Freshw. Biol. 51, 1389–1406.
Caissie, D., 2016. River evaporation, condensation and heat fluxes within a first-order tributary of Catamaran Brook (New Brunswick, Canada). Hydrol. Process. 30, 1872–1883.
Caissie, D., Luce, C.H., 2017. Quantifying streambed advection and conduction heat fluxes. Water Resour. Res. 53, 1595–1624.
Capell, R., Tetzlaff, D., Soulsby, C., 2013. Will catchment characteristics moderate the projected effects of climate change on flow regimes in the Scottish Highlands? Hydrol. Process. 27, 687–699.
Chen, Y.D., Carsel, R.F., McCutcheon, S.C., Nutter, W.L., 1998. Stream temperature simulation of forested riparian areas: I. Watershed-Scale Model Development. J. Environ. Eng. 124, 304–315.
Crisp, D.T., 1997. Water temperature of Plynlimon streams. Hydrol. Earth Syst. Sci. 1, 535–540.
Dickson, N.E., Carrivick, J.L., Brown, L.E., 2012. Flow regulation alters alpine river thermal regimes. J. Hydrol. 464–465, 505–516.
Dosskey, M.G., Vidon, P., Gurwick, N.P., Allan, C.J., Duval, T.P., Lowrance, R., 2010. The role of riparian vegetation in protecting and improving chemical water quality in Streams1. J. Am. Water Resour. Assoc. 46, 261–277.
Drainey, N., 2012. Tree Scheme to Put Salmon in Shade. The Times (February 6th, 2012).
Dugdale, S.J., Bergeron, N.E., St-Hilaire, A., 2015. Spatial distribution of thermal refuges analysed in relation to riverscape hydromorphology using airborne thermal infrared imagery. Remote Sens. Environ. 160, 43–55.
Dugdale, S.J., Franssen, J., Corey, E., Bergeron, N.E., Lapointe, M., Cunjak, R.A., 2016. Main stem movement of Atlantic salmon parr in response to high river temperature. Ecol. Freshw. Fish 25, 429–445.
Dunham, J.B., Rosenberger, A.E., Luce, C.H., Rieman, B.E., 2007. Influences of wildfire and channel reorganization on spatial and temporal variation in stream temperature and the distribution of fish and amphibians. Ecosystems 10, 335–346.
EA, 2011. Keeping Rivers Cool: Getting Ready for Climate Change by Creating Riparian Shade. Environment Agency, Bristol, UK.
Evans, E.C., McGregor, G.R., Petts, G.E., 1998. River energy budgets with special reference to river bed processes. Hydrol. Process. 12, 575–595.
Ficke, A., Myrick, C., Hansen, L., 2007. Potential impacts of global climate change on freshwater fisheries. Rev. Fish Biol. Fish. 17, 581–613.
Forestry Commission Scotland, 2006. The Scottish Forestry Strategy. Forestry Commission Scotland (The Scottish Executive), Edinburgh, UK (88 pp.).
Forestry Commission Scotland, 2015. National Forest Inventory Woodland Scotland 2015. Edinburgh, UK: Forestry Commission Scotland (The Scottish Executive) Dataset available online. https://data.gov.uk/dataset/national-forest-inventory-woodland-gb-2015.
Frazer, G.W., Canham, C.D., Lertzman, K.P., 1999. Gap Light Analyzer (GLA), Version 2: Imaging Software to Extract Canopy Structure and Light Transmission Indices from True-Colour Fisheye Photographs, User's Manual and Program Documentation. Simon Fraser University, Burnaby, BC & Institute of Ecosystem Studies, Millbrook, NY (36 pp.).
García-Haro, F.J., Gilabert, M.A., Meliá, J., 1999. A radiosity model for heterogeneous canopies in remote sensing. J. Geophys. Res. Atmos. 104, 12159–12175.
Gariglio, F.P., Tonina, D., Luce, C.H., 2013. Spatiotemporal variability of hyporheic exchange through a pool-riffle-pool sequence. Water Resour. Res. 49, 7185–7204.
Garner, G., Malcolm, I.A., Sadler, J.P., Hannah, D.M., 2014. What causes cooling water temperature gradients in a forested stream reach? Hydrol. Earth Syst. Sci. 18, 5361–5376.
Garner, G., Malcolm, I.A., Sadler, J.P., Millar, C.P., Hannah, D.M., 2015. Inter-annual variability in the effects of riparian woodland on micro-climate, energy exchanges and water temperature of an upland Scottish stream. Hydrol. Process. 29, 1080–1095.
Garner, G., Malcolm, I.A., Sadler, J.P., Hannah, D.M., 2017. The role of riparian vegetation density, channel orientation and water velocity in determining river temperature dynamics. J. Hydrol. http://dx.doi.org/10.1016/j.jhydrol.2017.03.024 (In Press).
Guenther, S.M., Gomi, T., Moore, R.D., 2014. Stream and bed temperature variability in a coastal headwater catchment: influences of surface-subsurface interactions and partial-retention forest harvesting. Hydrol. Process. 28, 1238–1249.
Gurnell, A.M., Clark, M.J., Hill, C.T., 1992. Analysis and interpretation of patterns within and between hydroclimatological time series in an alpine glacier basin. Earth Surf. Process. Landf. 17, 821–839.
Hannah, D.M., Garner, G., 2015. River water temperature in the United Kingdom: changes over the 20th century and possible changes over the 21st century. Prog. Phys. Geogr. 39, 68–92.
Hannah, D.M., Malcolm, I.A., Soulsby, C., Youngson, A.F., 2004. Heat exchanges and temperatures within a salmon spawning stream in the Cairngorms, Scotland: seasonal and sub-seasonal dynamics. River Res. Appl. 20, 635–652.
Hannah, D.M., Malcolm, I.A., Soulsby, C., Youngson, A.F., 2008. A comparison of forest and moorland stream microclimate, heat exchanges and thermal dynamics. Hydrol. Process. 22, 919–940.
Harriman, R., Morrison, B.R.S., Birks, H.J.B., Christie, A.E.G., Collen, P., Wattb, A.W., 1995. Long-term chemical and biological trends in Scottish streams and lochs. Water Air Soil Pollut. 85, 701–706.
Harriman, R., Watt, A.W., Christie, A.E.G., Moore, D.W., McCartney, A.G., Taylor, E.M., 2003. Quantifying the effects of forestry practices on the recovery of upland streams and lochs from acidification. Sci. Total Environ. 310, 101–111.
Hefting, M.M., Clement, J.-C., Bienkowski, P., Dowrick, D., Guenat, C., Butturini, A., Topa, S., Pinay, G., Verhoeven, J.T.A., 2005. The role of vegetation and litter in the nitrogen dynamics of riparian buffer zones in Europe. Ecol. Eng. 24, 465–482.
Hrachowitz, M., Soulsby, C., Imholt, C., Malcolm, I.A., Tetzlaff, D., 2010. Thermal regimes in a large upland salmon river: a simple model to identify the influence of landscape controls and climate change on maximum temperatures. Hydrol. Process. 24, 3374–3391.
Imholt, C., Gibbins, C.N., Malcolm, I.A., Langan, S., Soulsby, C., 2010. Influence of riparian cover on stream temperatures and the growth of the mayfly *Baetis rhodani* in an upland stream. Aquat. Ecol. 44, 669–678.
Imholt, C., Soulsby, C., Malcolm, I.A., Gibbins, C.N., 2013. Influence of contrasting riparian forest cover on stream temperature dynamics in salmonid spawning and nursery streams. Ecohydrology 6, 380–392.
IPCC, 2013. Climate Change 2013: The Physical Science Basis. Contribution of Working Group I to the Fifth Assessment Report of the Intergovernmental Panel on Climate Change. Cambridge University Press, Cambridge, UK.
Jackson, F.L., Hannah, D.M., Fryer, R.J., Millar, C.P., Malcolm, I.A., 2017. Development of spatial regression models for predicting summer river temperatures from landscape characteristics: implications for land and fisheries management. Hydrol. Process. 31, 1225–1238.
Janisch, J.E., Wondzell, S.M., Ehinger, W.J., 2012. Headwater stream temperature: interpreting response after logging, with and without riparian buffers, Washington, USA. For. Ecol. Manag. 270, 302–313.
Jones, H.G., Vaughan, R.A., 2011. Remote Sensing of Vegetation: Principles, Techniques, and Applications. Oxford University Press, Oxford, UK.
Jonsson, B., Jonsson, N., 2009. A review of the likely effects of climate change on anadromous Atlantic salmon *Salmo salar* and brown trout *Salmo trutta*, with particular reference to water temperature and flow. J. Fish Biol. 75, 2381–2447.
Keith, R.M., Bjornn, T.C., Meehan, W.R., Hetrick, N.J., Brusven, M.A., 1998. Response of juvenile salmonids to riparian and instream cover modifications in small streams flowing through second-growth forests of Southeast Alaska. Trans. Am. Fish. Soc. 127, 889–907.
Kibler, K.M., Skaugset, A., Ganio, L.M., Huso, M.M., 2013. Effect of contemporary forest harvesting practices on headwater stream temperatures: initial response of the Hinkle Creek catchment, Pacific Northwest, USA. For. Ecol. Manag. 310, 680–691.
Konarska, J., Lindberg, F., Larsson, A., Thorsson, S., Holmer, B., 2014. Transmissivity of solar radiation through crowns of single urban trees—application for outdoor thermal comfort modelling. Theor. Appl. Climatol. 117, 363–376.
Kreutzweiser, D.P., Capell, S.S., Holmes, S.B., 2009. Stream temperature responses to partial-harvest logging in riparian buffers of boreal mixedwood forest watersheds. Can. J. For. Res. 39, 497–506.
Laizé, C.L.R., Hannah, D.M., 2010. Modification of climate–river flow associations by basin properties. J. Hydrol. 389, 186–204.
Lawrence, A., Dandy, N., 2014. Private landowners' approaches to planting and managing forests in the UK: What's the evidence? Land Use Policy 36, 351–360.
Leach, J.A., Moore, R.D., 2010. Above-stream microclimate and stream surface energy exchanges in a wildfire-disturbed riparian zone. Hydrol. Process. 24, 2369–2381.
Leach, J.A., Moore, R.D., 2014. Winter stream temperature in the rain-on-snow zone of the Pacific Northwest: influences of hillslope runoff and transient snow cover. Hydrol. Earth Syst. Sci. 18, 819–838.
Leach, J.A., Moore, R.D., Hinch, S.G., Gomi, T., 2012. Estimation of forest harvesting-induced stream temperature changes and bioenergetic consequences for cutthroat trout in a coastal stream in British Columbia, Canada. Aquat. Sci. 74, 427–441.
Lim, K., Treitz, P., Wulder, M., St-Onge, B., Flood, M., 2003. LiDAR remote sensing of forest structure. Prog. Phys. Geogr. 27, 88–106.
Lintunen, A., Kaitaniemi, P., Perttunen, J., Sievänen, R., 2013. Analysing species-specific light transmission and related crown characteristics of *Pinus sylvestris* and *Betula pendula* using a shoot-level 3D model. Can. J. For. Res. 43, 929–938.
Lowe, S., Repper, N., Miles, L., Wallace, S., 2012. Notes on Tree Planting and the use of Native Species in North east England. Northumberland Wildlife Trust, Newcastle-upon-Tyne, UK.
Maheu, A., Caissie, D., St-Hilaire, A., El-Jabi, N., 2014. River evaporation and corresponding heat fluxes in forested catchments. Hydrol. Process. 28 (23), 5725–5738.
Malcolm, I.A., Hannah, D.M., Donaghy, M.J., Soulsby, C., Youngson, A.F., 2004. The influence of riparian woodland on the spatial and temporal variability of stream water temperatures in an upland salmon stream. Hydrol. Earth Syst. Sci. 8, 449–459.
Malcolm, I.A., Soulsby, C., Hannah, D.M., Bacon, P.J., Youngson, A.F., Tetzlaff, D., 2008. The influence of riparian woodland on stream temperatures: implications for the performance of juvenile salmonids. Hydrol. Process. 22, 968–979.
Malcolm, I.A., Gibbins, C.N., Fryer, R.J., Keay, J., Tetzlaff, D., Soulsby, C., 2014. The influence of forestry on acidification and recovery: insights from long-term hydrochemical and invertebrate data. Ecol. Indic. 37 (Part B), 317–329.

Martins, E.G., Hinch, S.G., Patterson, D.A., Hague, M.J., Cooke, S.J., Miller, K.M., Robichaud, D., English, K.K., Farrell, A.P., 2012. High river temperature reduces survival of sockeye salmon (*Oncorhynchus nerka*) approaching spawning grounds and exacerbates female mortality. Can. J. Fish. Aquat. Sci. 69, 330–342.
McCartney, A.G., Harriman, R., Watt, A.W., Moore, D.W., Taylor, E.M., Collen, P., Keay, E.J., 2003. Long-term trends in pH, aluminium and dissolved organic carbon in Scottish fresh waters; implications for brown trout (*Salmo trutta*) survival. Sci. Total Environ. 310, 133–141.
Moore, R.D., Spittlehouse, D.L., Story, A., 2005a. Riparian microclimate and stream temperature response to forest harvesting: a review. J. Am. Water Resour. Assoc. 41, 813–834.
Moore, R.D., Sutherland, P., Gomi, T., Dhakal, A., 2005b. Thermal regime of a headwater stream within a clear-cut, coastal British Columbia, Canada. Hydrol. Process. 19, 2591–2608.
Morin, G., Couillard, D., 1990. Chapter 5: Predicting river temperatures with a hydrological model. In: Cheremisinoff, N. (Ed.), Encyclopedia of Fluid Mechanics: Surface and Groundwater Flow Phenomena. Gulf Publishing, Houston, TX, pp. 171–209.
Morrill, J., Bales, R., Conklin, M., 2005. Estimating stream temperature from air temperature: implications for future water quality. J. Environ. Eng. 131, 139–146.
Orr, H.G., Johnson, M.F., Wilby, R.L., Hatton-Ellis, T., Broadmeadow, S., 2015. What else do managers need to know about warming rivers? A United Kingdom perspective. WIRES 2, 55–64.
Ouellet, V., Secretan, Y., St-Hilaire, A., Morin, J., 2014. Water temperature modelling in a controlled environment: comparative study of heat budget equations. Hydrol. Process. 28, 279–292.
Parrott, J., Holbrook, J., 2006. Natural Heritage Trends: riparian woodlands in Scotland – 2006. Scottish Natural Heritage Commissioned Report No. 204 (ROAME No. F01NB02a). Scottish National Heritage, Inverness, UK.
Pollock, M.M., Beechie, T.J., Liermann, M., Bigley, R.E., 2009. Stream temperature relationships to forest harvest in Western Washington1. J. Am. Water Resour. Assoc. 45, 141–156.
Punzet, M., Voß, F., Voß, A., Kynast, E., Bärlund, I., 2012. A global approach to assess the potential impact of climate change on stream water temperatures and related in-stream first-order decay rates. J. Hydrometeorol. 13, 1052–1065.
Rios, S.L., Bailey, R.C., 2006. Relationship between riparian vegetation and stream benthic communities at three spatial scales. Hydrobiologia 553, 153–160.
Rishel, G.B., Lynch, J.A., Corbett, E.S., 1982. Seasonal stream temperature changes following forest harvesting. J. Environ. Qual. 11, 112–116.
Roth, T.R., Westhoff, M.C., Huwald, H., Huff, J.A., Rubin, J.F., Barrenetxea, G., Vetterli, M., Parriaux, A., Selker, J.S., Parlange, M.B., 2010. Stream temperature response to three riparian vegetation scenarios by use of a distributed temperature validated model. Environ. Sci. Technol. 44, 2072–2078.
Rouquette, J.R., Thompson, D.J., 2005. Habitat associations of the endangered damselfly, Coenagrion mercuriale, in a water meadow ditch system in southern England. Biol. Conserv. 123, 225–235.
Rowe, L.K., Pearce, A.J., O'Loughlin, C.L., 1994. Hydrology and related changes after harvesting native forest catchments and establishing pinus radiata plantations. Part 1. Introduction to study. Hydrol. Process. 8, 263–279.
Stott, T., Marks, S., 2000. Effects of plantation forest clearfelling on stream temperatures in the Plynlimon experimental catchments, mid-Wales. Hydrol. Earth Syst. Sci. 4, 95–104.
Tetzlaff, D., Malcolm, I.A., Soulsby, C., 2007. Influence of forestry, environmental change and climatic variability on the hydrology, hydrochemistry and residence times of upland catchments. J. Hydrol. 346, 93–111.
Tetzlaff, D., Brewer, M.J., Malcolm, I.A., Soulsby, C., 2010. Storm flow and baseflow response to reduced acid deposition—using Bayesian compositional analysis in hydrograph separation with changing end members. Hydrol. Process. 24, 2300–2312.
van Vliet, M.T.H., Ludwig, F., Zwolsman, J.J.G., Weedon, G.P., Kabat, P., 2011. Global river temperatures and sensitivity to atmospheric warming and changes in river flow. Water Resour. Res. 47, W02544.
van Vliet, M.T.H., Franssen, W.H.P., Yearsley, J.R., Ludwig, F., Haddeland, I., Lettenmaier, D.P., Kabat, P., 2013. Global river discharge and water temperature under climate change. Glob. Environ. Chang. 23, 450–464.
Webb, B.W., 1996. Trends in stream and river temperature. Hydrol. Process. 10, 205–226.
Webb, B.W., Crisp, D.T., 2006. Afforestation and stream temperature in a temperate maritime environment. Hydrol. Process. 20, 51–66.
Webb, B.W., Zhang, Y., 1997. Spatial and seasonal variability in the components of the river heat budget. Hydrol. Process. 11, 79–101.
Webb, B.W., Zhang, Y., 1999. Water temperatures and heat budgets in Dorset chalk water courses. Hydrol. Process. 13, 309–321.
Webb, B.W., Zhang, Y., 2004. Intra-annual variability in the non-advective heat energy budget of Devon streams and rivers. Hydrol. Process. 18, 2117–2146.
Webb, B.W., Hannah, D.M., Moore, R.D., Brown, L.E., Nobilis, F., 2008. Recent advances in stream and river temperature research. Hydrol. Process. 22, 902–918.
Welles, J.M., Norman, J.M., 1991. Instrument for indirect measurement of canopy architecture. Agron. J. 83, 818–825.
Wirth, L., Rosenberger, A., Prakash, A., Gens, R., Margraf, F.J., Hamazaki, T., 2012. A remote-sensing, GIS-based approach to identify, characterize, and model spawning habitat for fall-run chum salmon in a sub-arctic, glacially fed river. Trans. Am. Fish. Soc. 141, 1349–1363.
Withrow-Robinson, B.A., Bennett, M., Ahrens, G.R., 2011. A Guide to Riparian Tree and Shrub Planting in the Willamette Valley: Steps to Success. Oregon State University Extension Service, Corvallis, OR.
Yearsley, J.R., 2009. A semi-Lagrangian water temperature model for advection-dominated river systems. Water Resour. Res. 45, W12405.
Zwieniecki, M.A., Newton, M., 1999. Influence of streamside cover and stream features on temperature trends in forested streams of western Oregon. West. J. Appl. For. 14, 106–113.